Functional Glasses: Properties And Applications for Energy and Information

Proceedings

Winter 1-10-2013

Surface Interactions on Glass Optics During Fabrication, Post Processing & Laser Operation

Tayyab Suratwala
Lawrence Livermore National Laboratory

Recommended Citation

Tayyab Suratwala, "Surface Interactions on Glass Optics During Fabrication, Post Processing & Laser Operation" in "Functional Glasses: Properties And Applications for Energy and Information", H. Jain, Lehigh Univ.; C. Pantano, The Pennsylvania State Univ.; S. Ito, Tokyo Institute of Technology; K. Bange, Schott Glass (ret.); D. Morse, Corning Eds, ECI Symposium Series, (2013). http://dc.engconfintl.org/functional_glasses/15

Surface interactions on glass optics during fabrication, post processing & laser operation

Functional Glasses: Properties and Applications for Energy & Information
Siracusa, Sicily, Italy

Friday, January 11, 2013
Keynote Presentation
Tayyab Suratwala

LLNL-PRES-608293-DRAFT

This work performed under the auspices of the U.S. Department of Energy by Lawrence Livermore National Laboratory under Contract DE-AC52-07NA27344

High-peak-power and high-average-power lasers demand laser damage resistant optics

Fusion Energy

- National Ignition Facility (NIF)
- Mercury Laser
- Laser Inertial Fusion Energy (LIFE)
- Laser MegaJoule (LMJ)
- Laboratory Laser Energetics (LLE)
- Etc….

Directed Energy

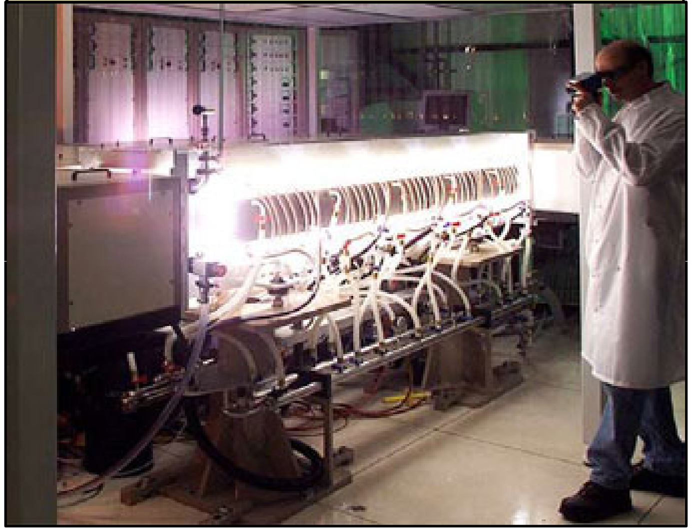

- High-Average-Power Laser (HAPL)
- Diode-pumped, solid-state heat-capacity laser (SSHCL)
- Tailored-aperture ceramic laser (TACL)

Commercial Lasers

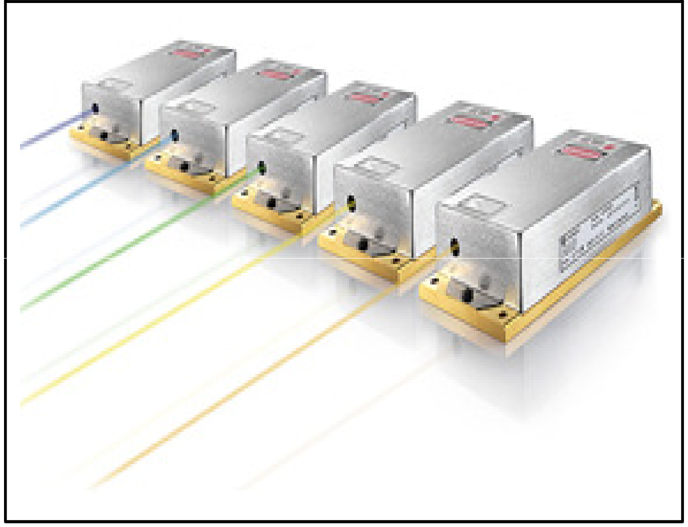

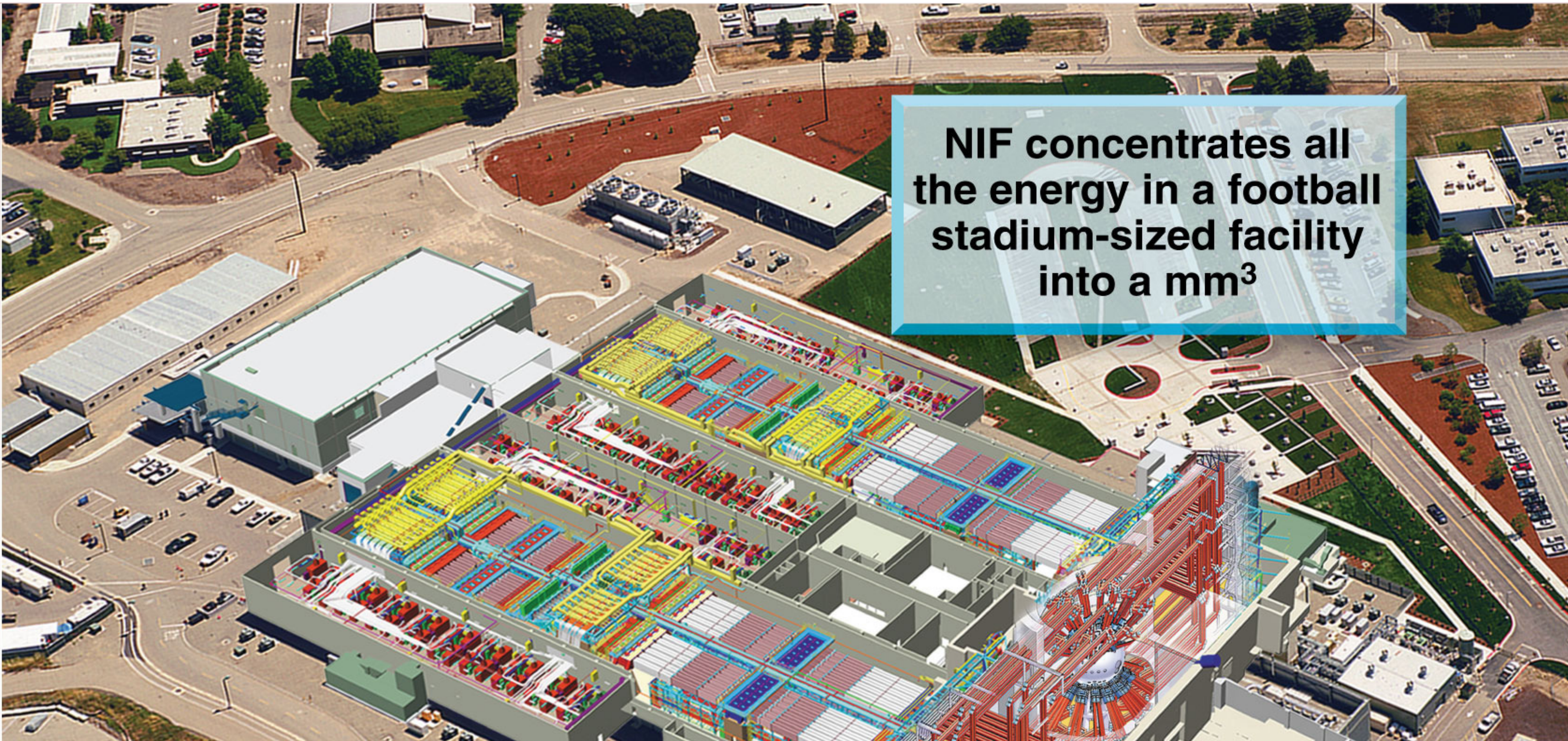

NIF concentrates all the energy in a football stadium-sized facility into a mm^3

Matter Temperature	$>10^8$ K
Radiation Temperature	$>3.5 \times 10^6$ K
Densities	$>10^3$ g/cm^3
Pressures	$>10^{11}$ atm

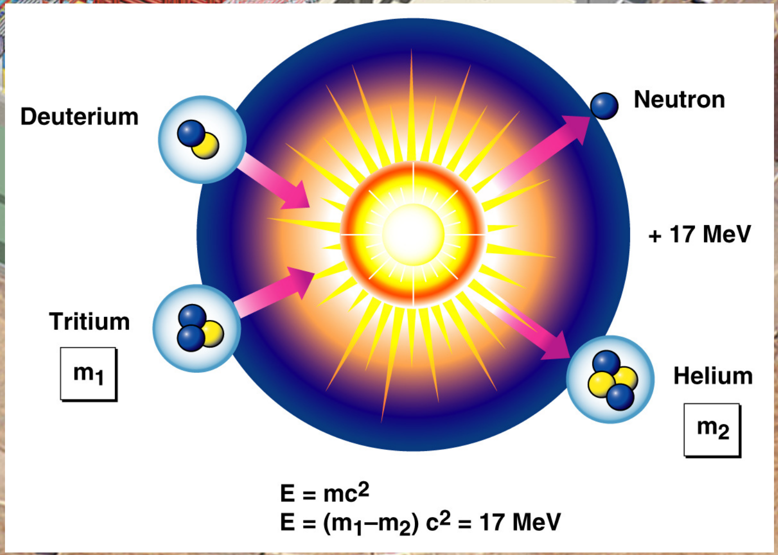

$E = mc^2$

$E = (m_1 - m_2)\,c^2 = 17$ MeV

Materials for NIF large optics are limited only to four different glasses or single crystals

KDP

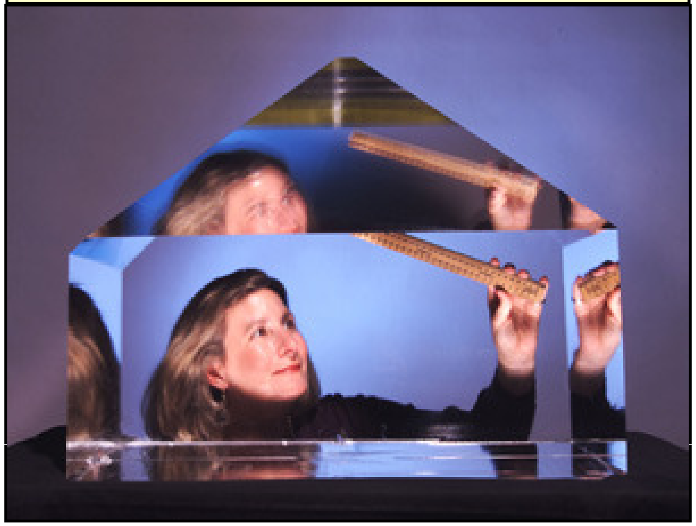

Laser Phosphate Glass

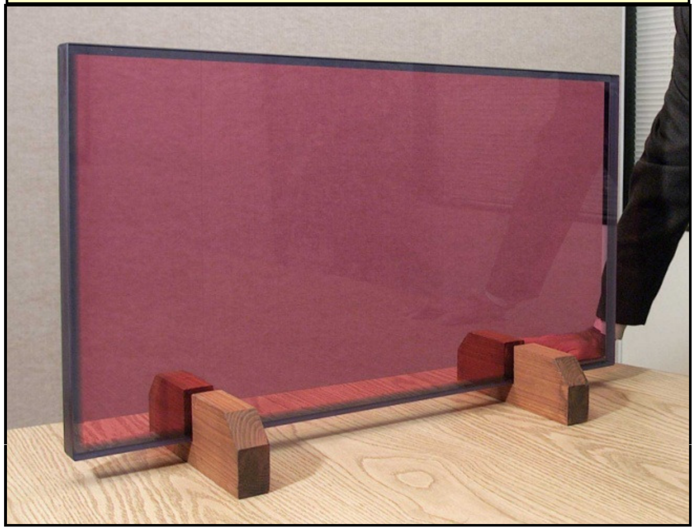

Fused Silica

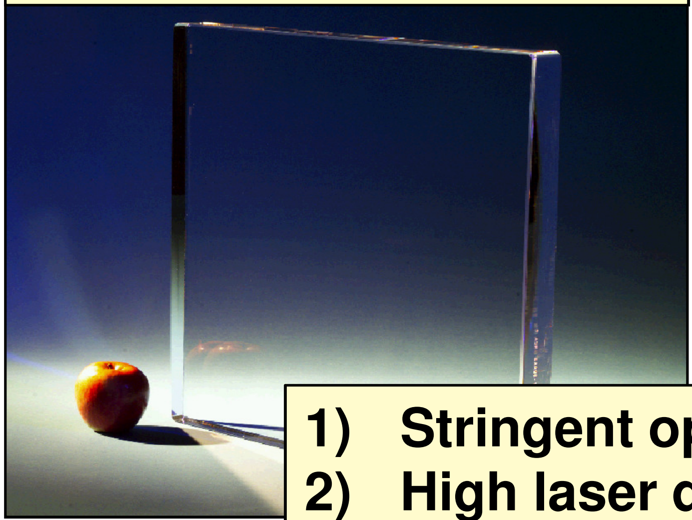

Borosilicate Glass

1) Stringent optical requirements
2) High laser damage resistance
3) Manufacturability to 0.5 m size scale

NIF's operational fluence & power have increased dramatically, strongly supported by more damage resistant optics

NIF can operate ~10x higher in fluence than previous lasers

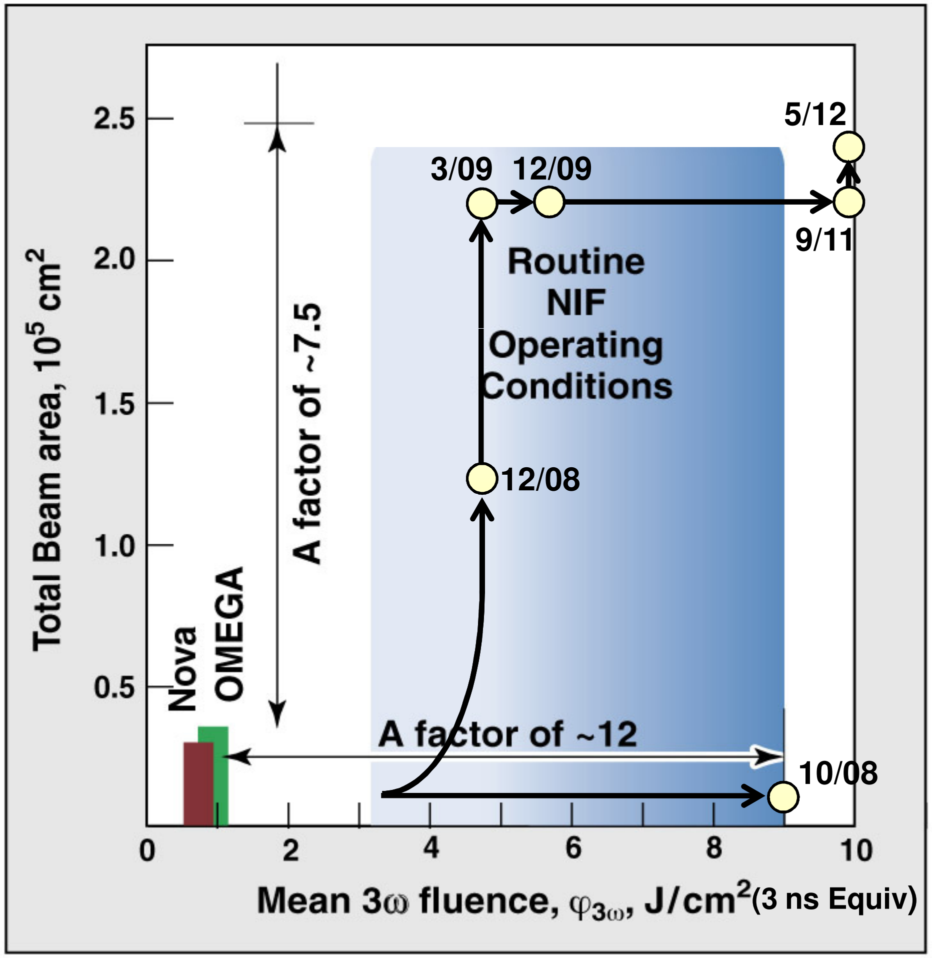

NIF's 3ω power has been increasing at a rate of 100TW/year

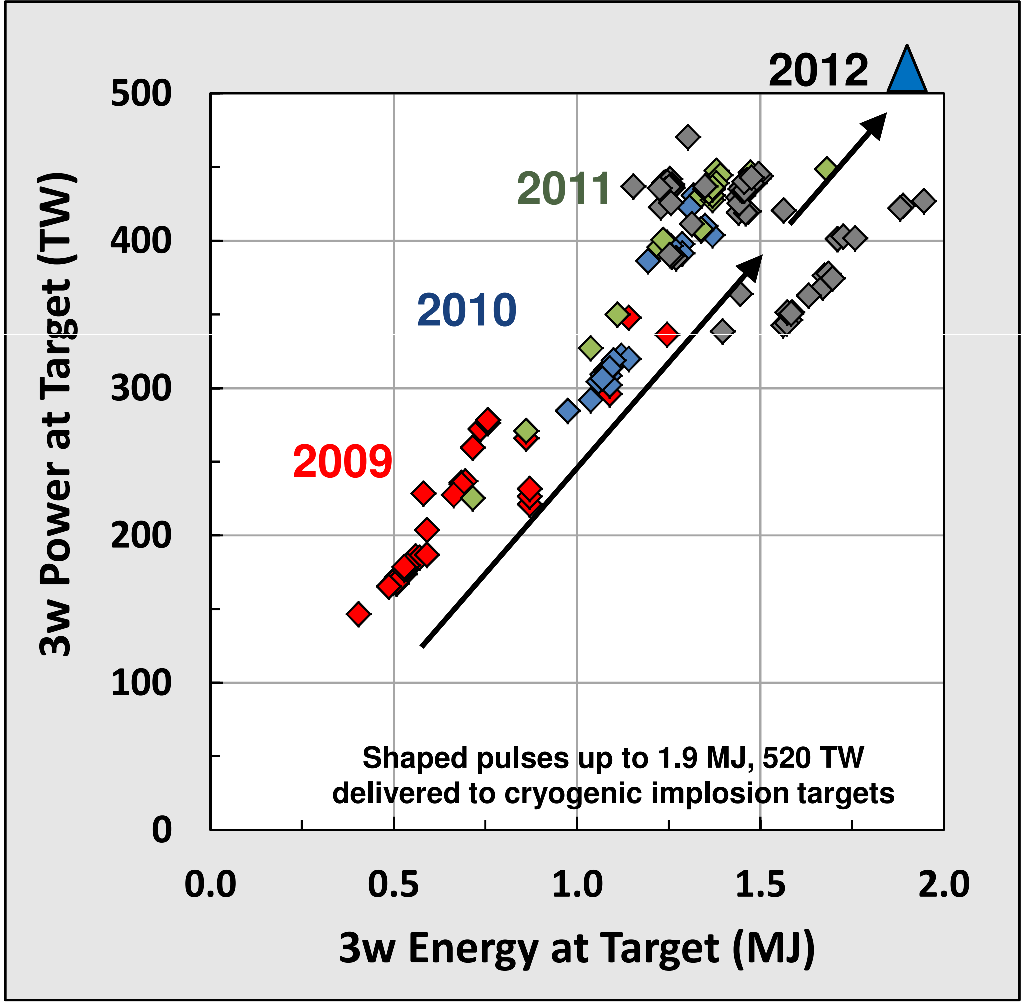

Greater understanding glass surface interactions has led to greatly improved high fluence glass optics

Optic improvement from 1997 to the present

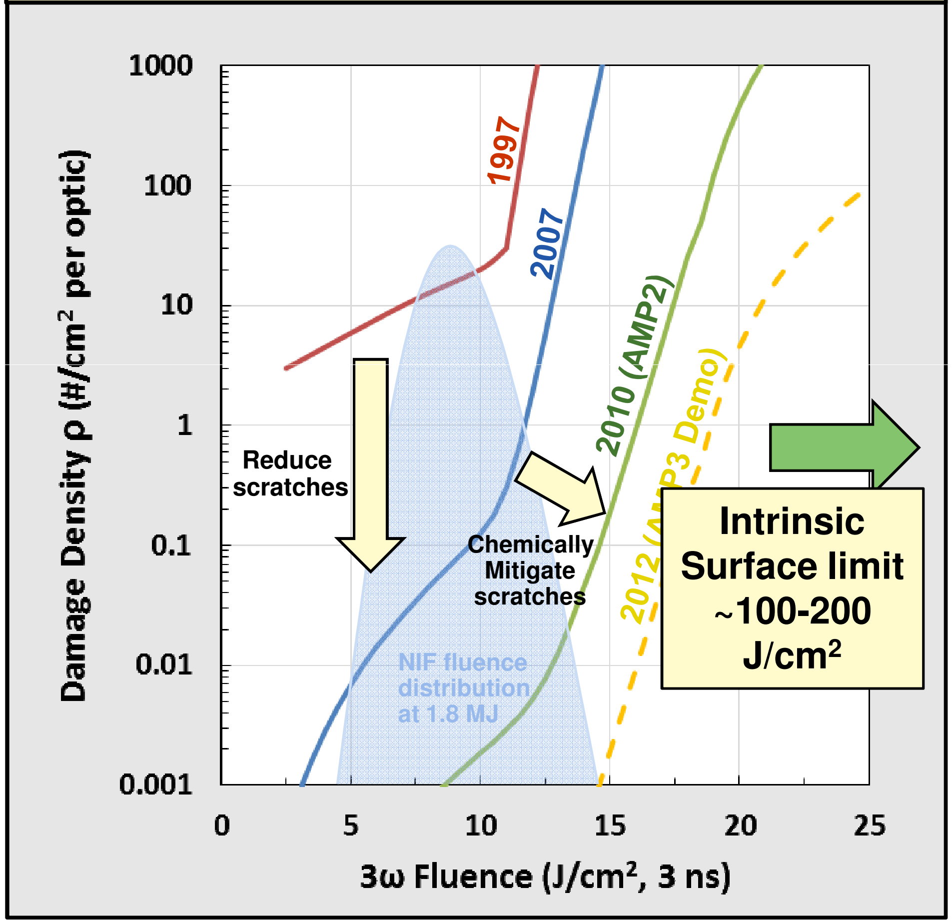

- ρ(φ) is the expected density of initiated sites as a function of 3ω illuminating fluence
- ρ(φ) is the metric used to describe the quality of the surface finish
  - Better optics have a lower ρ(φ)
- Greater than 4 orders of magnitude improvement from 1997 to present
  - Fracture reduction in conventional polishing
  - Chemical treatment to make residual fractures benign

Even today, there is much opportunity to increase surface damage threshold of glass surfaces

Our S&T has focused on understanding surface interactions on glass surfaces during fabrication, post processing and laser operation

	1. Optical Fabrication	2. Post Processing & Coatings	3. Laser Operation
Current Efforts	• Sub-surface damage management • Forensics of surface fractures • Fundamentals of material removal • Technology of full aperture & small tool optical finishing • Low cost, precursor-free finishing techniques	• Development of chemical/thermal-based flaw/damage mitigation • Development of laser-based flaw/damage mitigation • Laser interference gratings development	• Mechanism of initiation & growth (precursors & modulation) • Precursor isolation & identification • Quantitative understanding initiation & growth behavior • Understanding solarization effects • Understanding modulation effects

Various types of microscopic laser damage are observed on high fluence glass optics

Type A:
Gray Haze

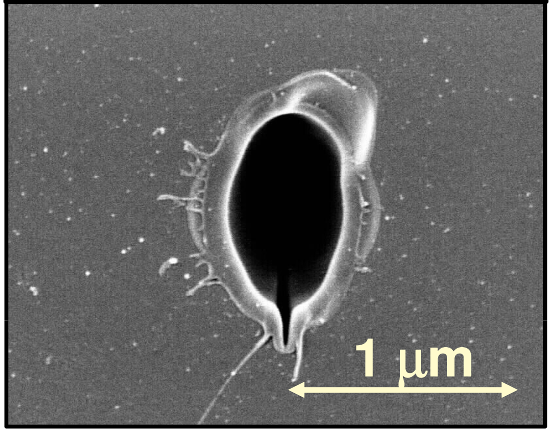

Type B:
Single/double lateral

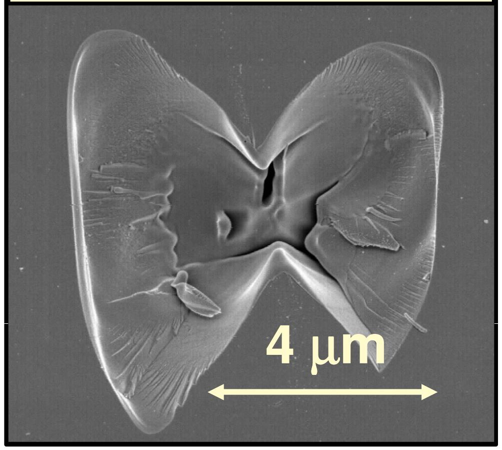

Pits from nodular ejection

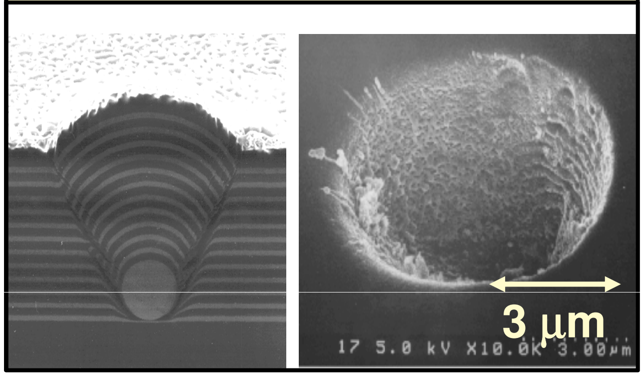

Delaminates

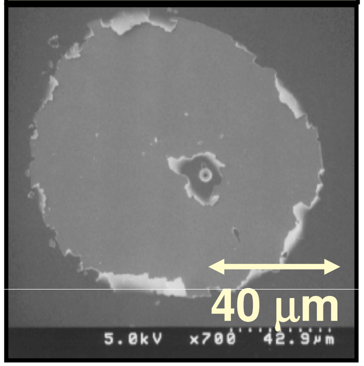

Type C: Classic

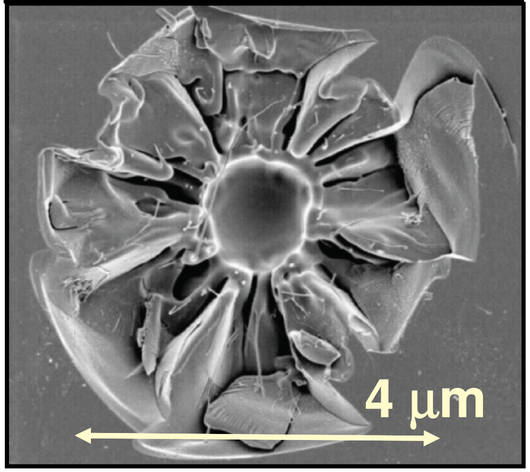

Type D: Shallow Sites

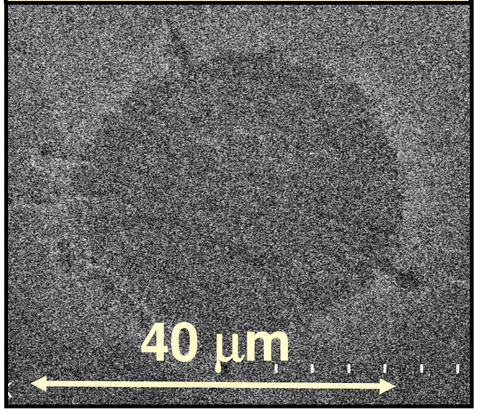

Flat bottom pits

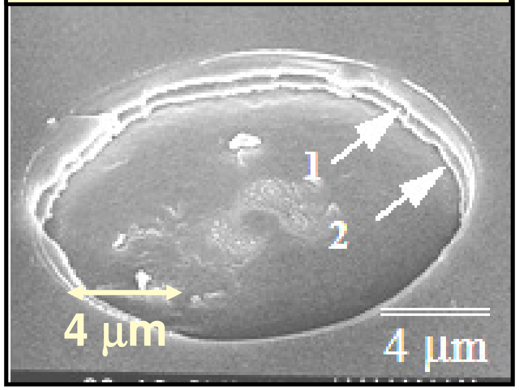

Plasma scalds

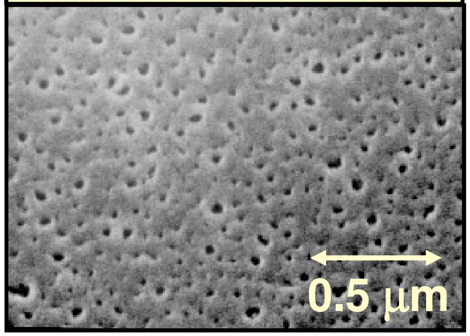

W. Carr, SPIE 6403, K1-9 (2007); Génin SPIE 2870, 439-448 (1996);

Many of these damage sites can grow larger with subsequent laser shots

Surface initiation of small damage sites

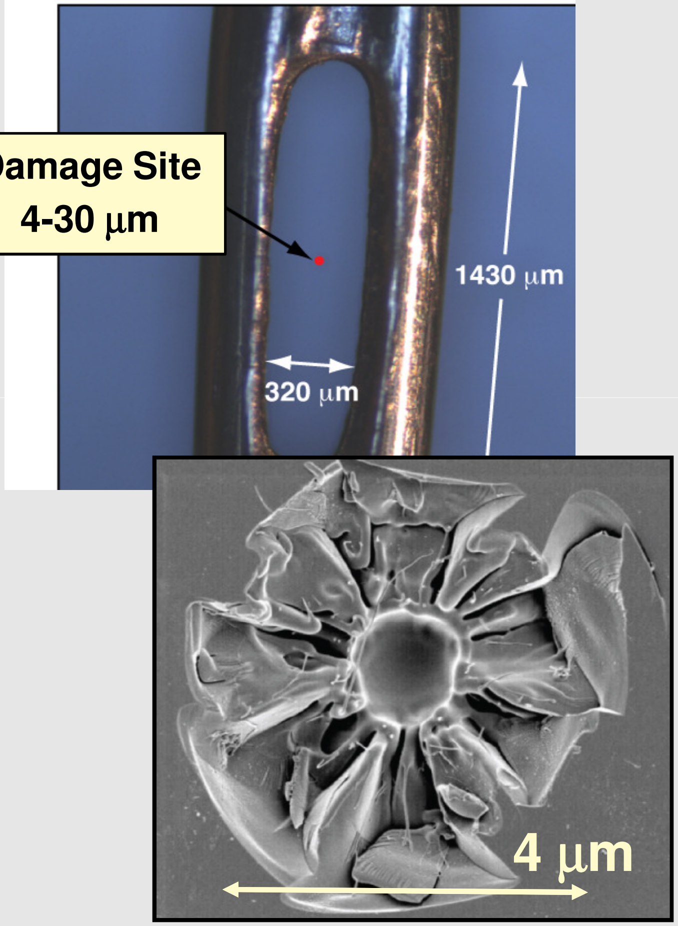

Damage Site
4-30 µm

16J/cm^2 355nm on fused silica

Damage initiates from sub-band gap absorbing precursors

Growth occurs at low fluence

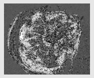

4-30 µm

Multiple laser shots (7 J/cm^2 351 nm)

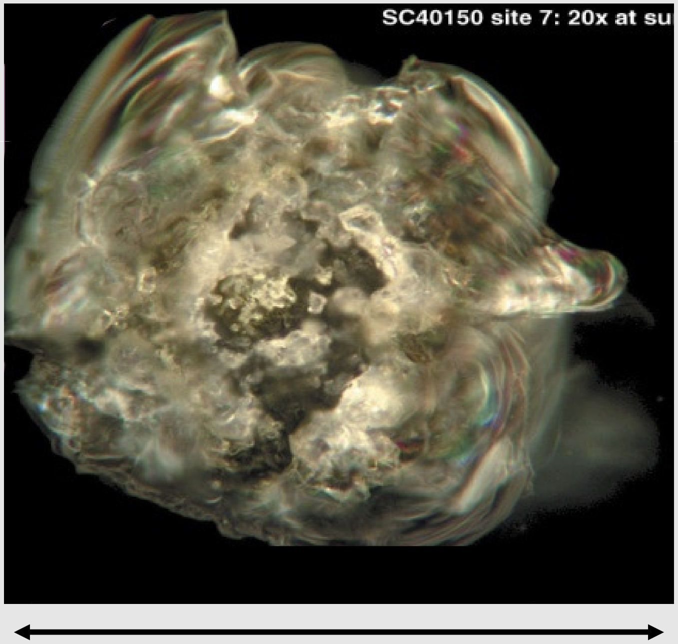

300 µm

Growth utimately limits optic’s lifetime

Laser damage mechanism:
T-activated absorption results in the formation of a laser-driven solid-state absorption front (AF)

Schematic of AF Model:
Lattice Temperature vs. depth

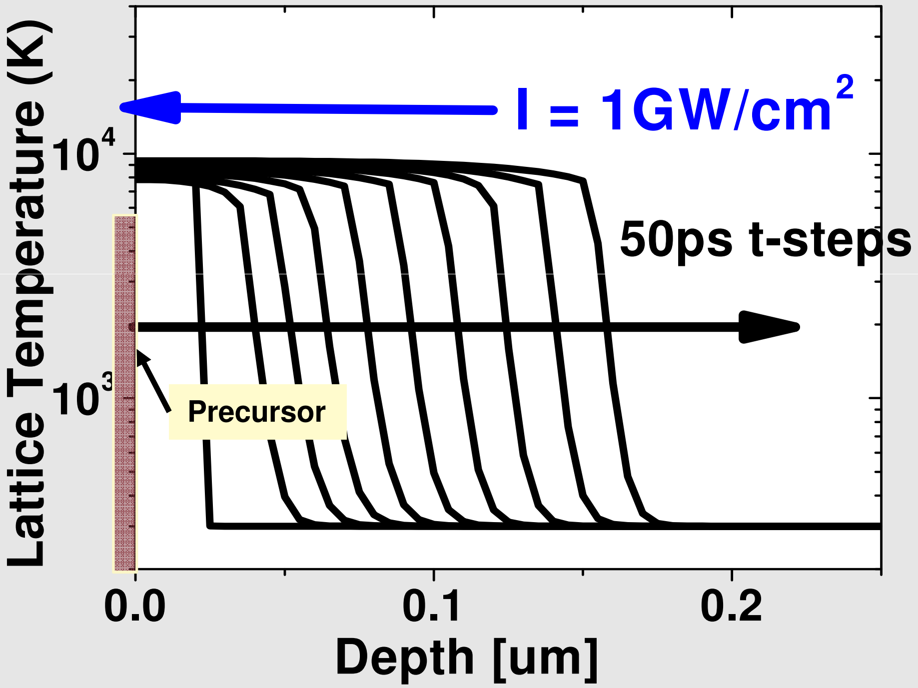

1. Near surface precursor is heated by absorption of laser light
2. T-activated bulk absorption, $\alpha_{INT}(T)$: precursor heats the bulk which begins to absorb (thermal runaway)
3. T-activated thermal conduction
4. Absorption front forms and propagates at velocity v_f

Fracture surfaces (not plastic deformation and densification) are low fluence absorbing precursors

0.5N Vickers Indent | **5 min BOE etch** | **0.1 N Knoop** | **0.5 N MRF removal**

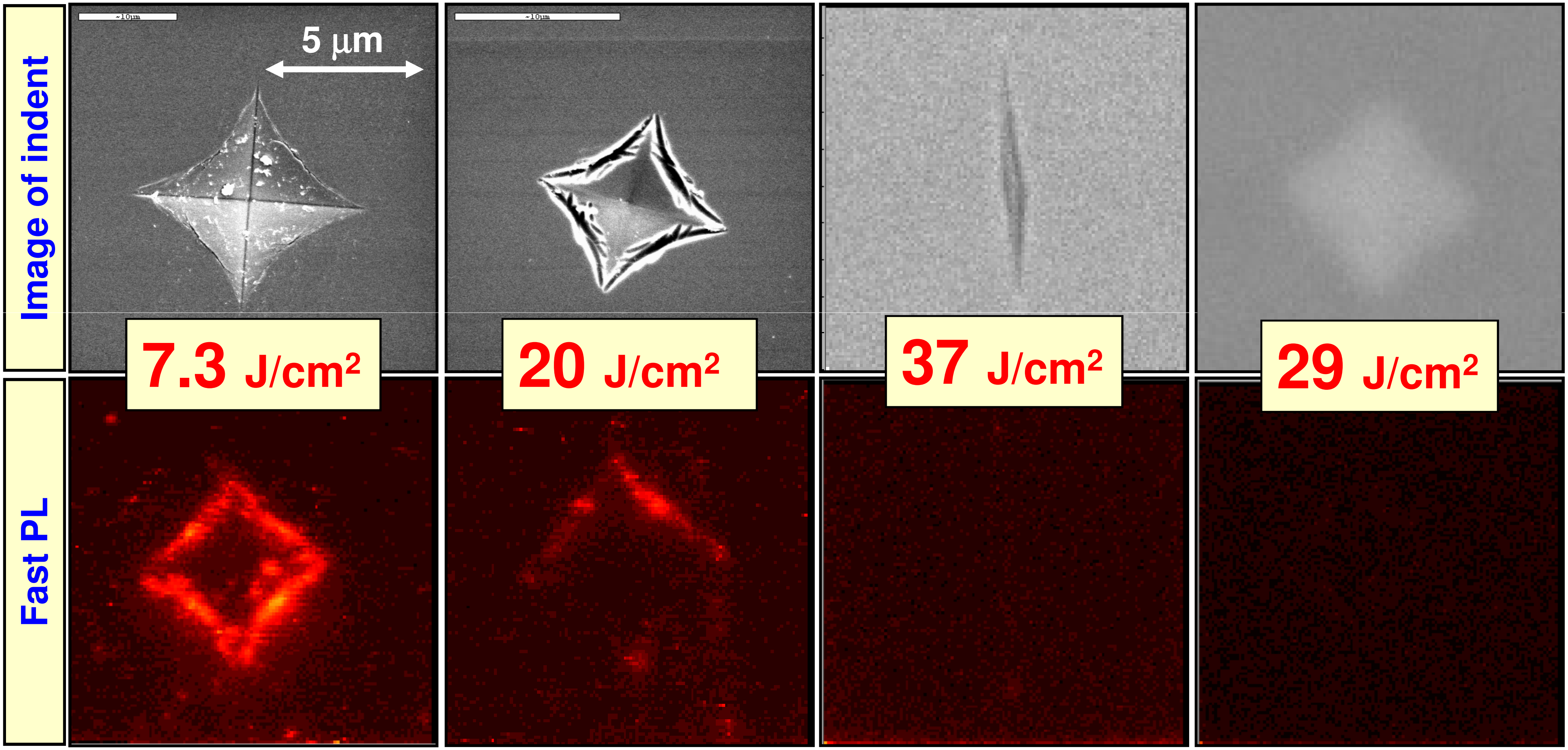

Fracture surface removed

No cracks; only plastic deformation

Densification only

P. Miller et al., Optics Letters 35 (16) 2010; T. Laurence, et al., APL 94, 151114 2009

Removal of subsurface impurities within the ‘Beilby’ polishing layer using HNO_3:H_2O_2 improves laser damage resistance

Ce surface concentration profile on fused silica with and without etching

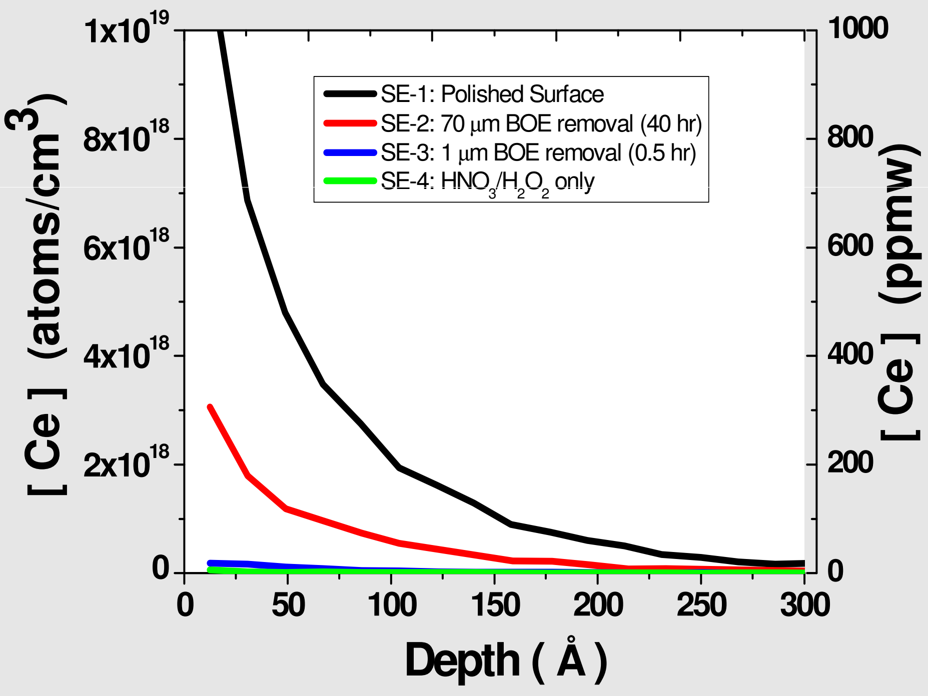

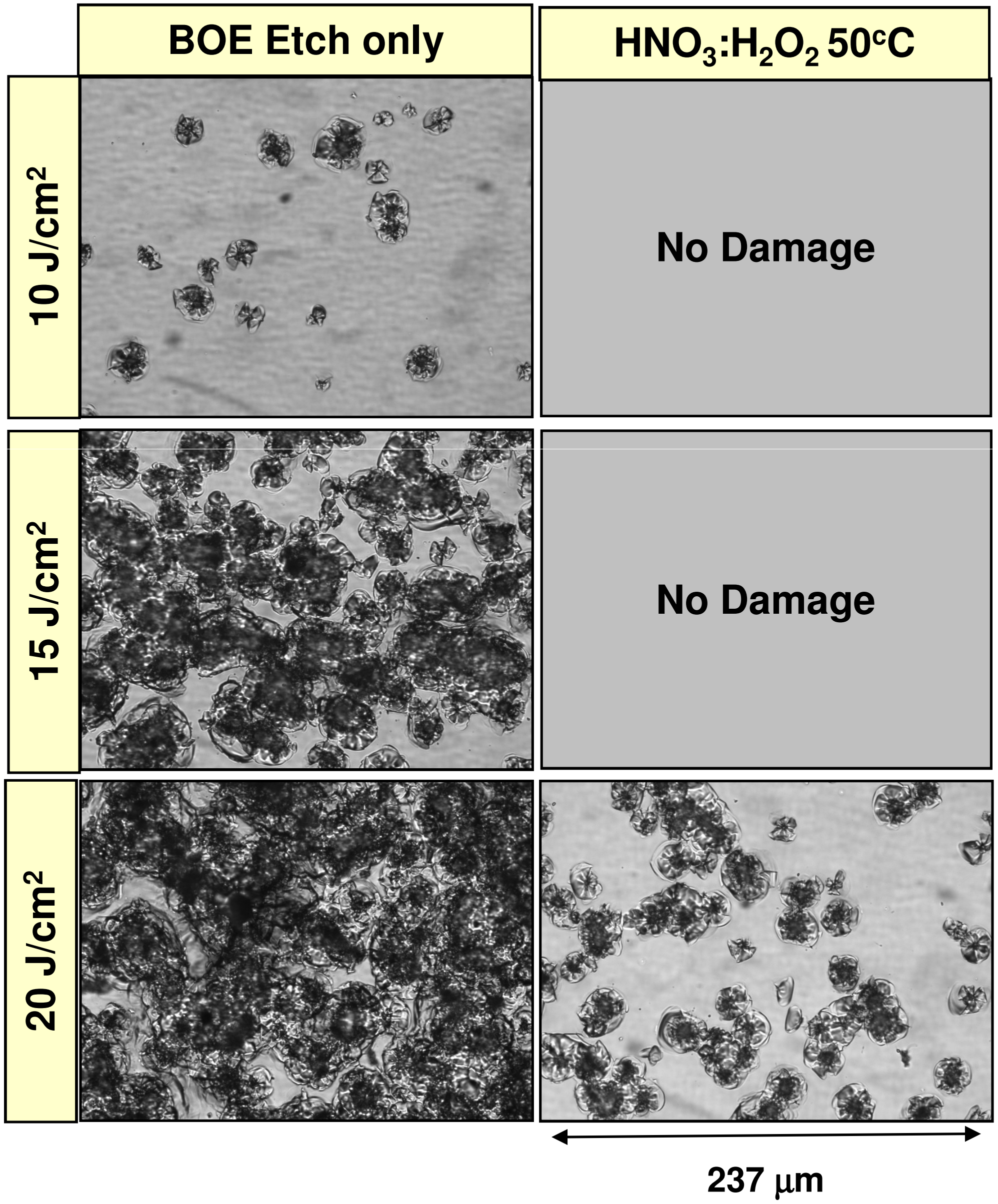

P. Miller, et. al. *US Patent 8,313,662* (11/20/12)

Three precursors on fused silica surface have been identified to lead to 3ω laser damage

Physical model of laser damage pre-cursors on fused silica

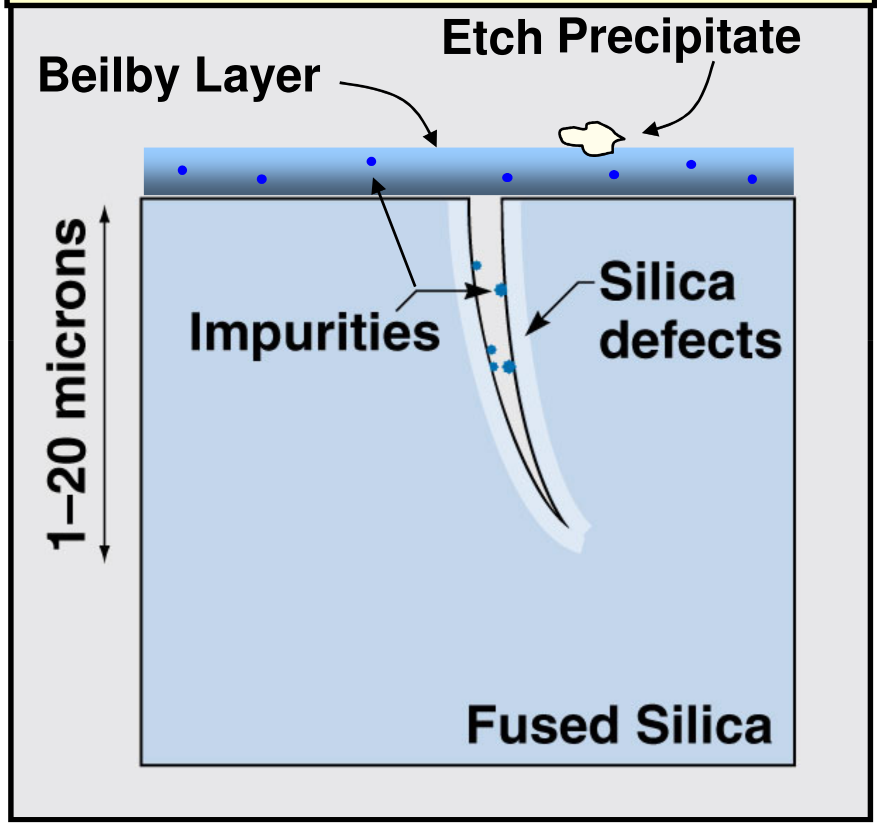

1) CHEMICAL IMPURITIES such as Ce in the Beibly layer and in fractures

2) INSTRINSIC SILICA DEFECTS ON FRACTURE SURFACES (e.g. scratches)

3) PRECIPITATION PRODUCTS which can result from subsequent surface treatments (e.g. CO_2 laser, chemical etching)

P. Miller, Optics Letters 35(16) (2010) 2702

Our S&T has focused on understanding surface interactions on glass surfaces during fabrication, post processing and laser operation

	1. Optical Fabrication	2. Post Processing & Coatings	3. Laser Operation
Current Efforts	• Sub-surface damage management • Forensics of surface fractures • Fundamentals of material removal • Technology of full aperture & small tool optical finishing • Low cost, precursor-free finishing techniques	• Development of chemical/thermal-based flaw/damage mitigation • Development of laser-based flaw/damage mitigation • Laser interference gratings development	• Mechanism of initiation & growth (precursors & modulation) • Precursor isolation & identification • Quantitative understanding initiation & growth behavior • Understanding solarization effects • Understanding modulation effects
Future Challenges			• Higher fluence precursor identification & mitigation • Understand multi-pulse surface & radiation effects • Understand/mitigating debris-induced damage • Understand damage mechanisms on other glass optics (including coatings) • Development of new glass optical materials (e.g., high fluence optical filters)

There are three basic types of cracks created by static brittle indentation

	Hertzian Cracks[1] (blunt)	**Radial Cracks[1] (sharp)**	**Lateral Cracks[2] (sharp)**
	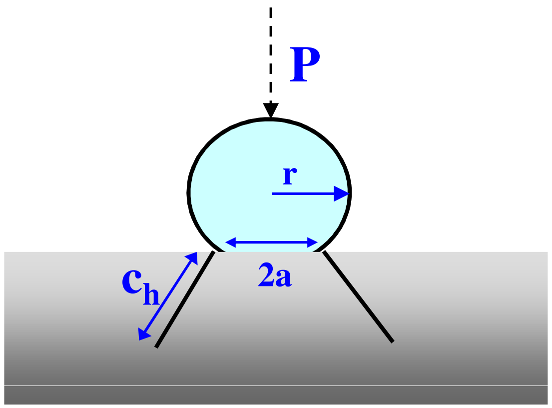	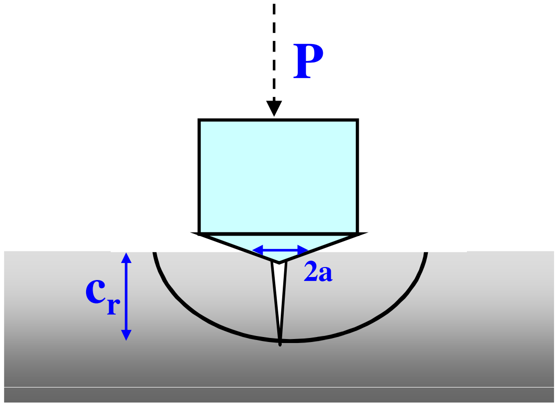	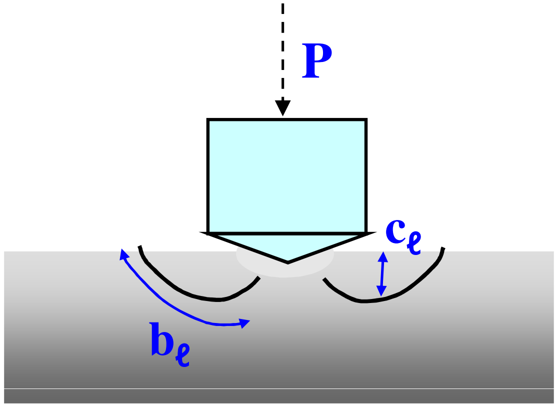
Initiation	$P_c = A\,r$	$P_c = \alpha_r \dfrac{K_{Ic}^4}{H^3}$	$P_c = P_{c\ell}$
Growth	$c_h = \left(\dfrac{\chi_h P}{K_{Ic}}\right)^{2/3}$	$c_r = \left(\dfrac{\chi_r P}{K_{Ic}}\right)^{2/3}$	$b_\ell = \dfrac{\chi_\ell \left(\dfrac{E}{H}\right)^{3/5} P^{5/8}}{K_{Ic}^{1/2} H^{1/8}}$ $c_\ell = \dfrac{\chi_{\ell 2} \left(\dfrac{E}{H}\right)^{2/5} P^{1/2}}{H^{1/2}}$
	Leads to subsurface damage	**Leads to subsurface damage**	**Leads to material removal**

1. B. Lawn, "Fracture of Brittle Materials" (1993)
2. I. Hutchings "Tribology:Friction and Wear of Engineering Materials" (1992)

There are multiple types of scratches which can be divided into three basic categories

Plastic Abrasive Wear

Sleek

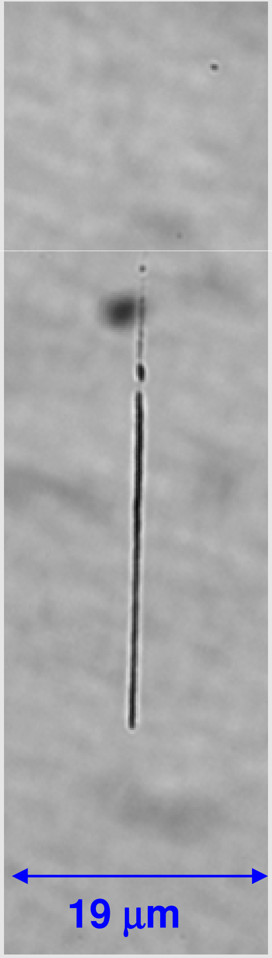

Mixed
Brittle fracture / Plastic Abrasive Wear

Sleek + lateral fracture

Sleek + trailing indent fracture

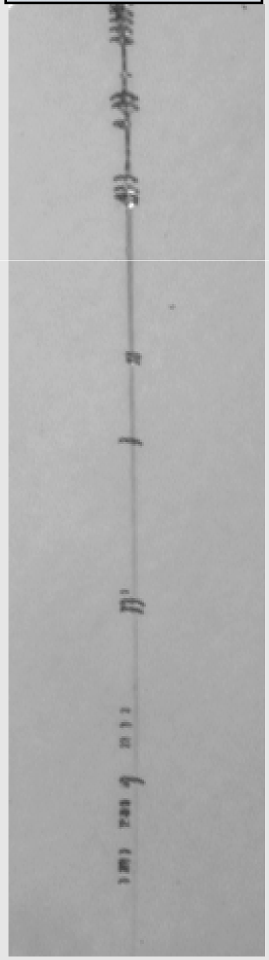

Sleek + trailing indent + lateral fracture

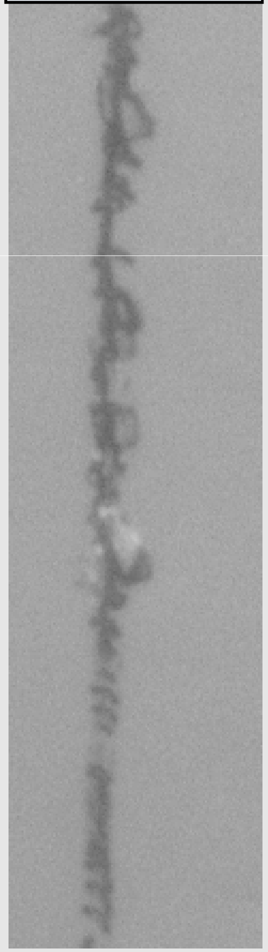

Brittle Fracture

Trailing indent fracture

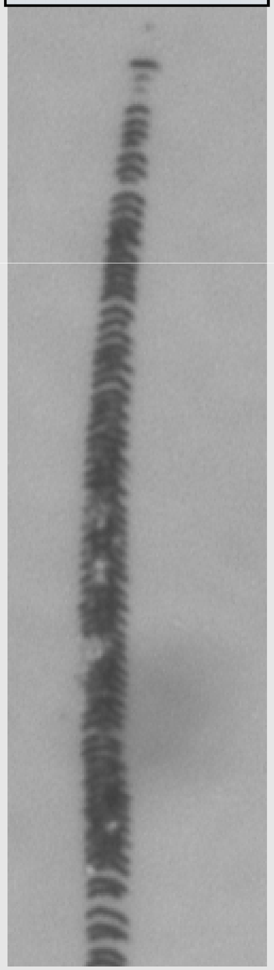

Trailing indent + lateral fracture

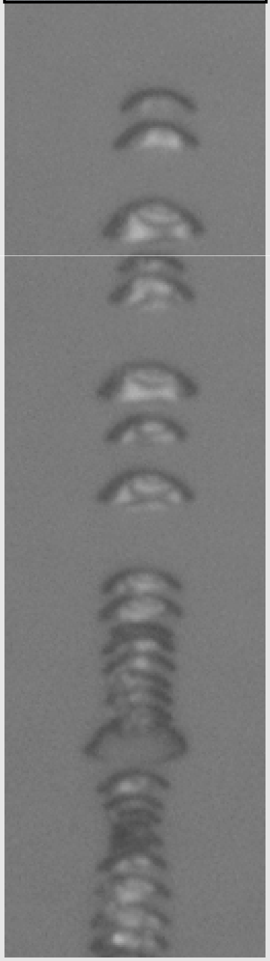

The MRF wedge technique is a useful method to <u>statistically</u> measure the SSD length and depth distribution

MRF Wedge Technique

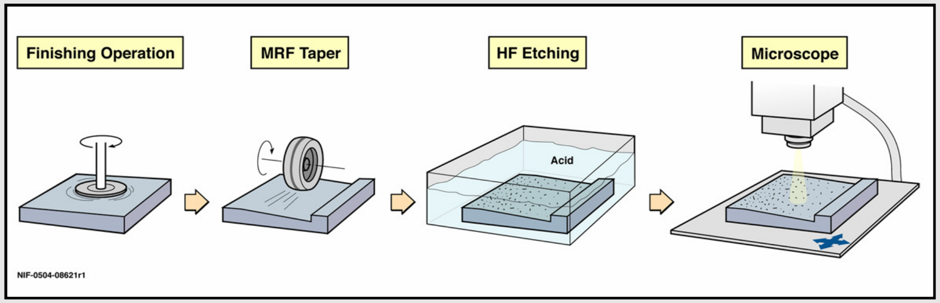

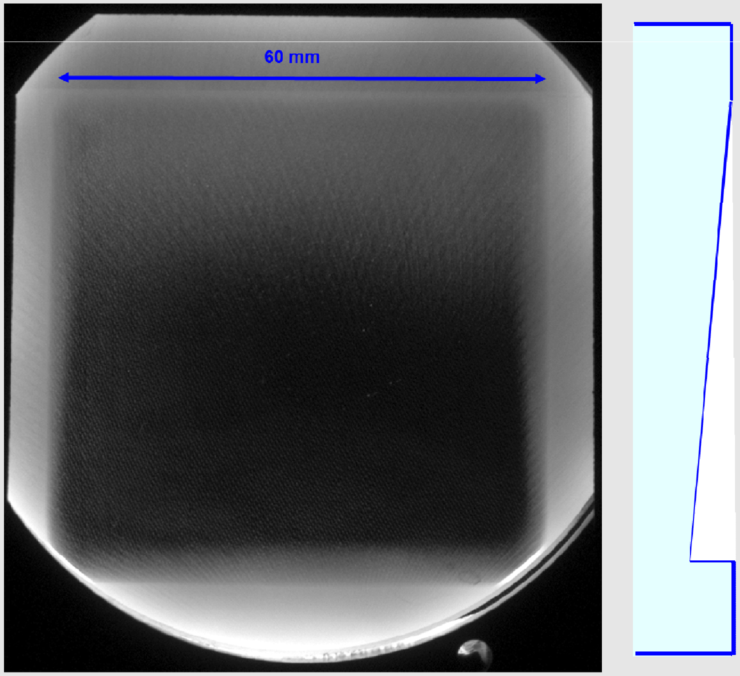

Measured Crack Depth Distributions

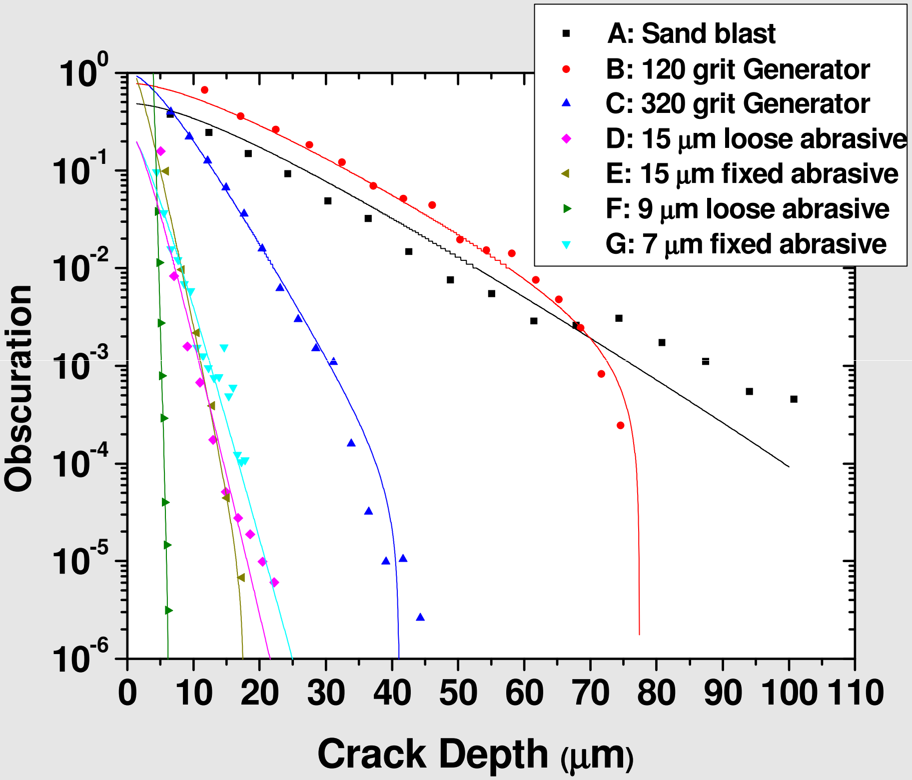

J. Menapace, *SPIE* 5991 (2005); T. Suratwala, JNCS 352 (2006) 5601

Microscope images of the fractures show a unique size character for each grinding step

Sand blasted

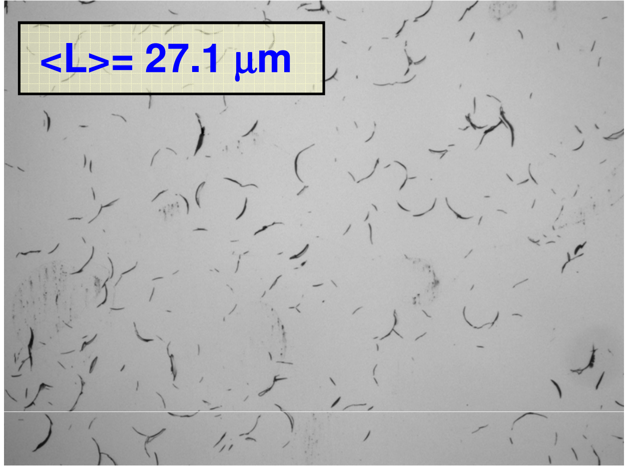

2.37 mm

120 Grit (125 µm)

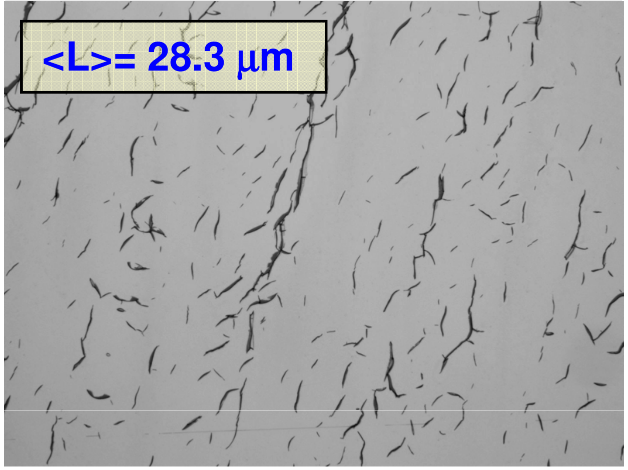

2.37 mm

150 Grit (100 µm)

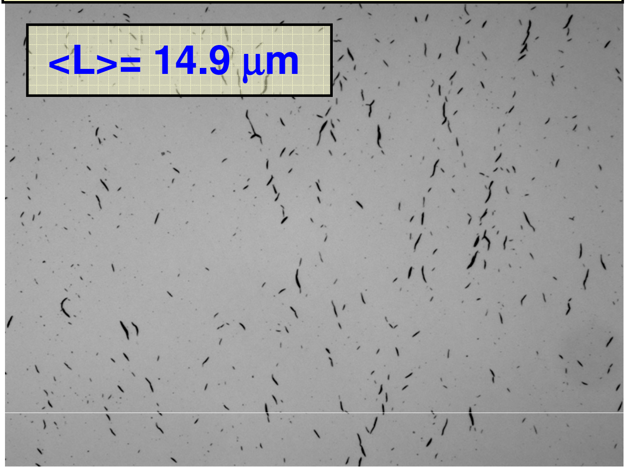

2.37 mm

15 µm loose abrasive

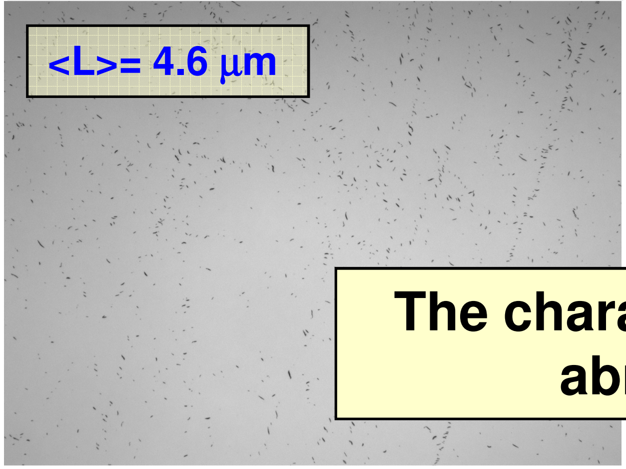

2.37 mm

15 µm fixed abrasive

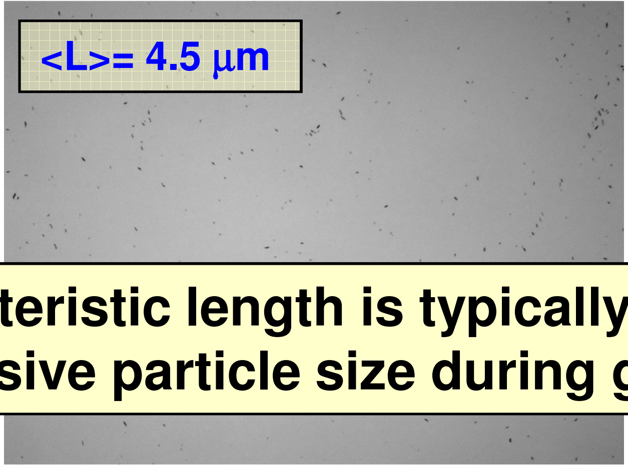

2.37 mm

9 µm loose abrasive

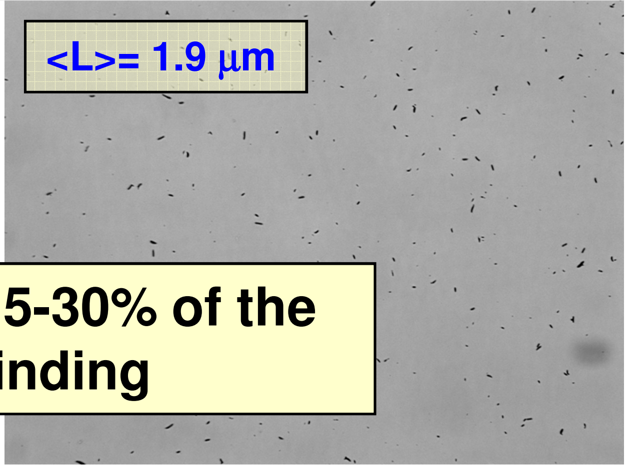

0.6 mm

The characteristic length is typically 15-30% of the abrasive particle size during grinding

A brittle fracture model has been successfully used to explain the observed distribution of crack depth and lengths

Schematic of Model*

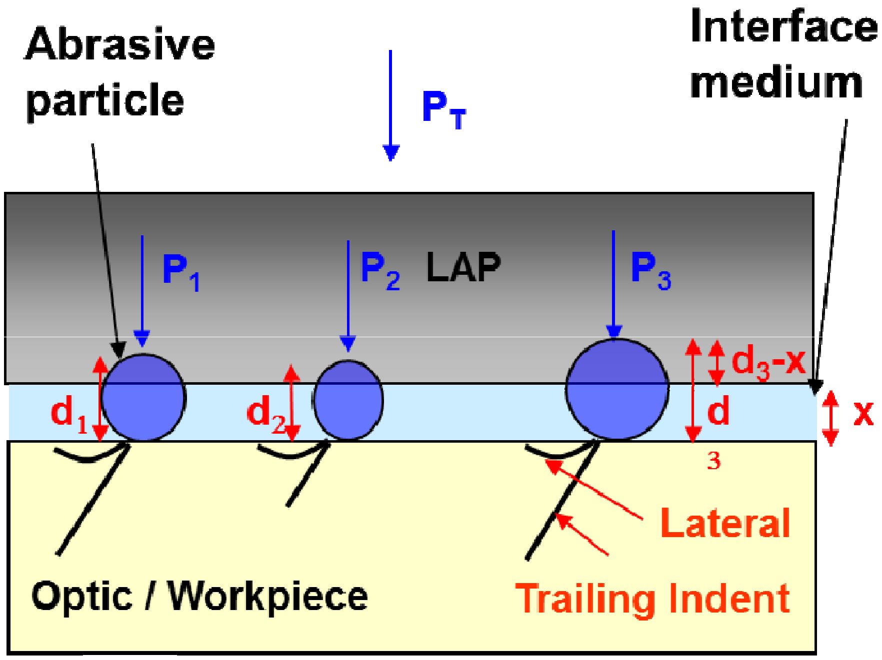

$P_T = \Sigma P_i$ $\qquad$ $P_i \propto (d_i - x) \propto d_i$

$$c(L) = \frac{L}{\frac{\pi}{2}\left(\frac{K_{Ic}}{\chi_h}\right)^{2/3}\left(\frac{2k\,N_L d_c}{3E\,P_T}\right)^{1/3}} = \frac{L}{\Omega}$$

$$c_{90} = 0.9 < L >$$

$$c_{\max} = 2.8 < L >$$

Key assumption: The load on particle is proportional to its vertical dimension

---

*T. Suratwala, JNCS 352 (2006) 5601. P. Miller, SPIE 5991 (2005).

During polishing large rogue particles or asperities bear high loads leading to sub-surface fractures (scratches)

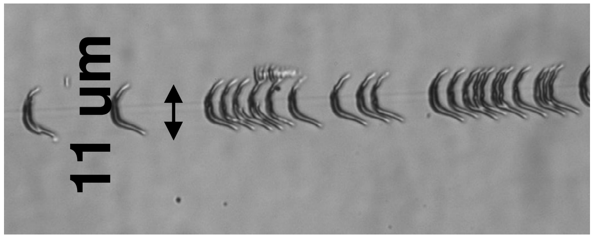

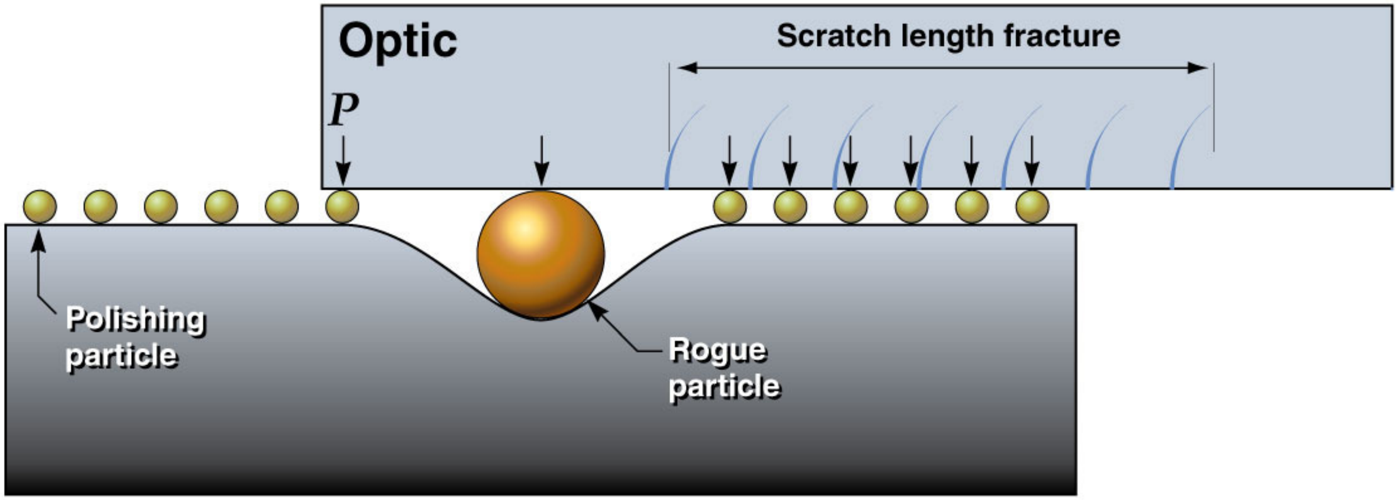

Viscoelastic Lap (Pitch or Pad)

- **Particle viscoelastically penetrates into pad**
- **Time frame of high load exposure determines scratch length**

$$L_{scratch} = 8.9 \frac{v_{ave} \eta R^2}{P}$$

T. Suratwala, et. al., JNCS 354 (2008) 2023

The scratch length correlates with viscoelastic model wrt rogue particle size, pressure, lap viscosity, and lap temperature

tt = 0 msec

Scratch length as a fn of various process parameters

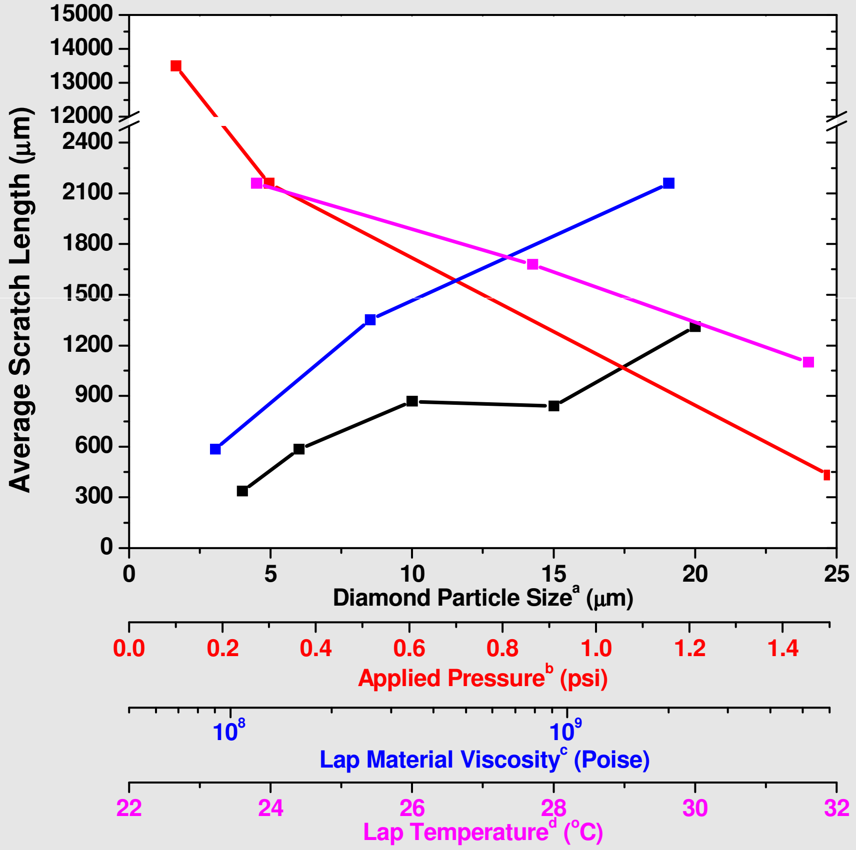

Simulation of rogue particle penetration

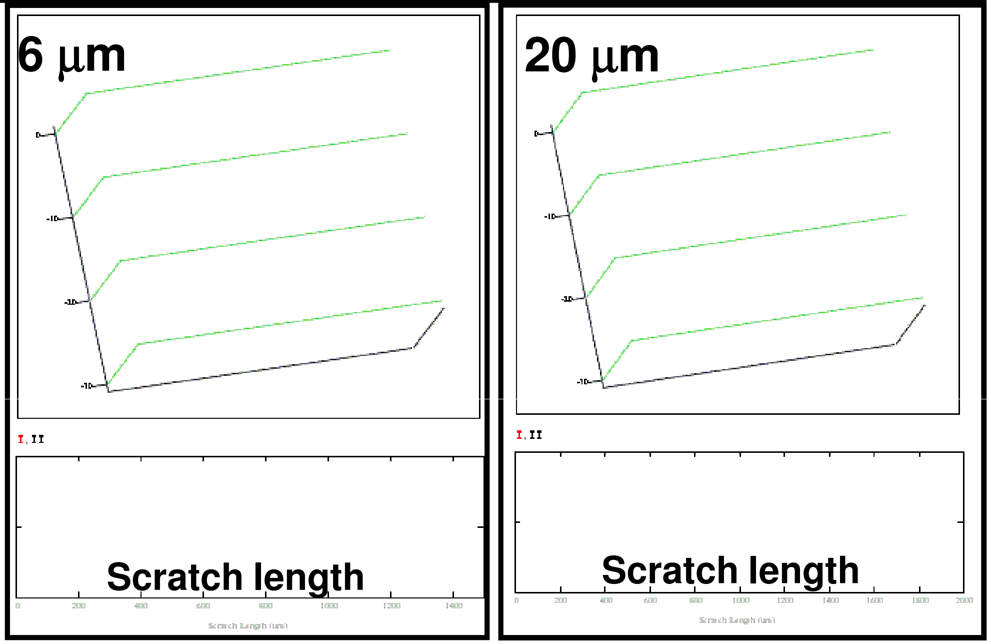

Viscoelastic Penetration Model Solution: Ting model solution modified by Feit

$$h=\begin{cases}\dfrac{a}{2}\log\left(\dfrac{R+a}{R-a}\right)-\left(R-\sqrt{R^2-r^2}\right) & for\ \ r<a\\[2ex] \left[\dfrac{a}{2}\log\left(\dfrac{R+a}{R-a}\right)-\left(R-\sqrt{R^2-a^2}\right)\right]\left(\left(1-\dfrac{1}{2}\left(\dfrac{r}{a}\right)^2\right)\sin^{-1}\left(\dfrac{a}{r}\right)+\dfrac{1}{2}\left(\left(\dfrac{r}{a}\right)^2-1\right)^{1/2}\right) & for\ \ r>a\end{cases}$$

T. Suratwala, et. al., JNCS 354 (2008) 2023

These studies have provided new rules that Opticians use to diagnose the cause of or to mitigate scratches

Property of scratch	What can it tell you?
1. Scratch width or trailing indent length (L)	- Size of rogue particle (d) - Size distribution of Rogue Particles - Process step - Depth of fracture (c_{90} or c_{max})
2. Number density	- Rogue particle concentration
3. Scratch length ($L_{scratch}$)	- Lap properties and rogue particle size
4. Scratch type (plastic, Brittle, mixed)	- Load during fracture - Sharpness of particle
5. Orientation and Pattern of trailing indent	- Particle movement direction - Particle rotation - Stick slip behavior
6. Curvature or scratch pattern	- Pathway of indenting particle - Shape of tool - Handling vs polishing
7. Location on optic	- Material removal & figure

Rule / Example

For grinding

$$0.15\,d \leq L \leq 0.3\,d$$

For polishing

$$0.3\,d \leq L \leq 0.5\,d$$

Sample	<L>
A: Sandblast	27.1 µm
B: 120 grit	28.3 µm
C: 320 grit	14.9 µm
D: 15 µm loose	4.6 µm
E: 15 µm fixed	4.5 µm
F: 9 µm loose	1.9 µm
G: 7 µm fixed	8.4 µm

$$c_{90} = 0.9 \langle L \rangle \quad c_{max} = 2.8 \langle L \rangle$$

$$\begin{aligned} &P \approx 0.001 - 0.1\,N && \textit{Plastic only} \\ &P \approx 0.1 - 5\,N && \textit{Plastic \& Brittle} \\ &P > 5\,N && \textit{Plastic \& rubble} \end{aligned}$$

$$L_{scratch} = 8.9\,\frac{v_{ave}\,\eta\,R^2}{P}$$

T. Suratwala, et. al., *Optics and Photonics News* (Sept 2008) 12.

HF etching can be used after grinding to remove subsurface fracture because it annihilates neighboring cracks

Etching a scratch

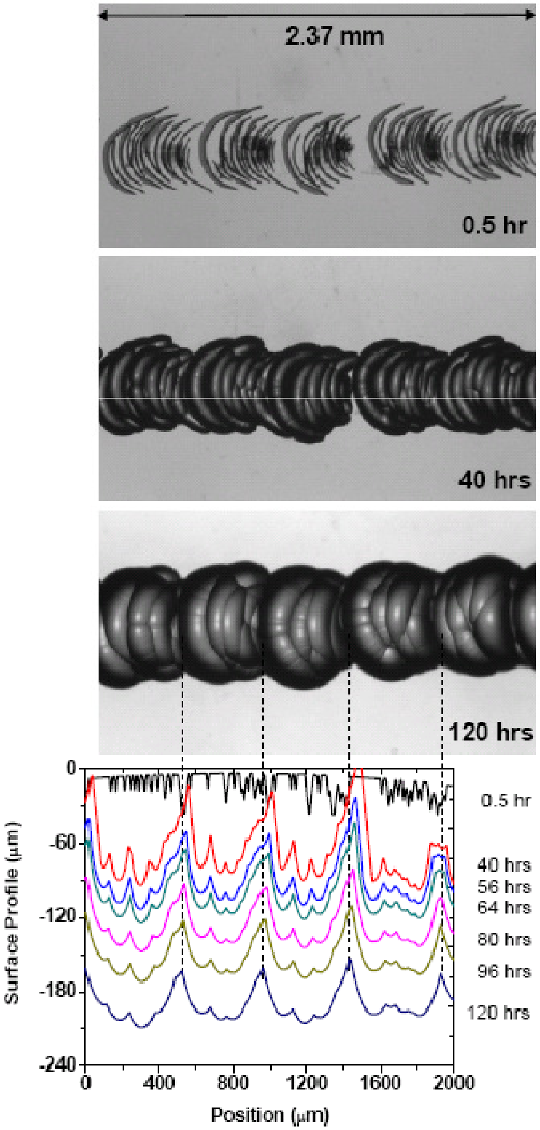

Etching ground surface

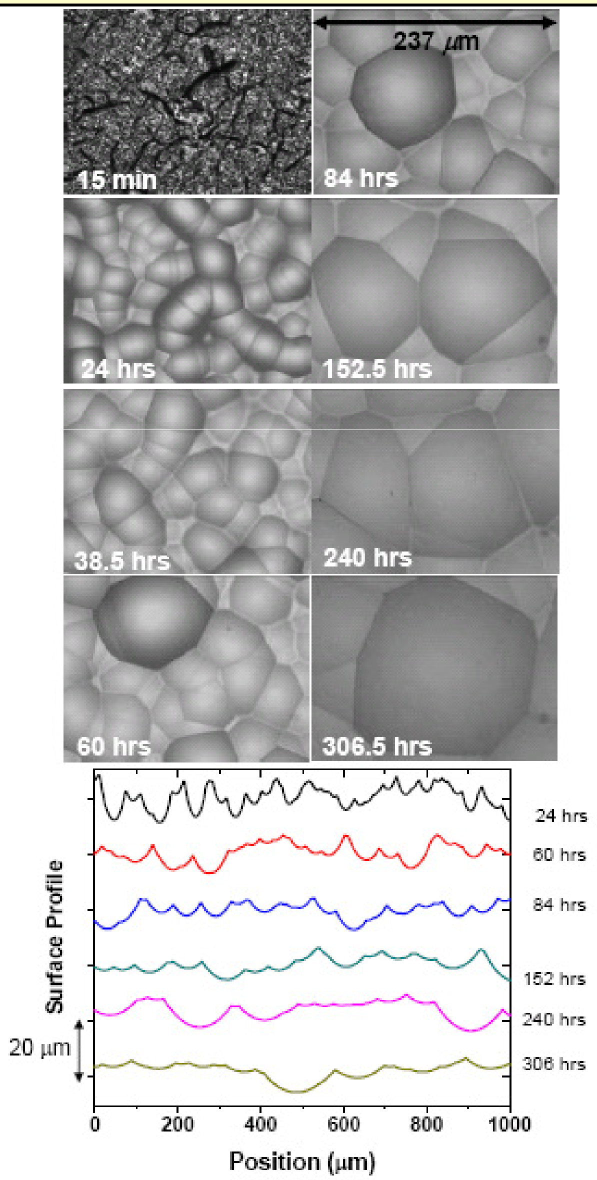

Simple Geometric Model

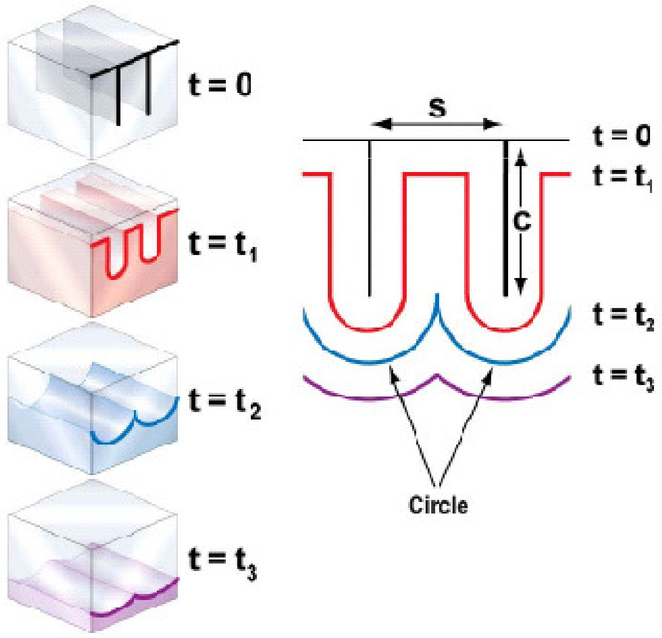

A finite difference etching model has been developed to determine optimum etching times and key process variables

Finite Difference Isotropic Etch Model

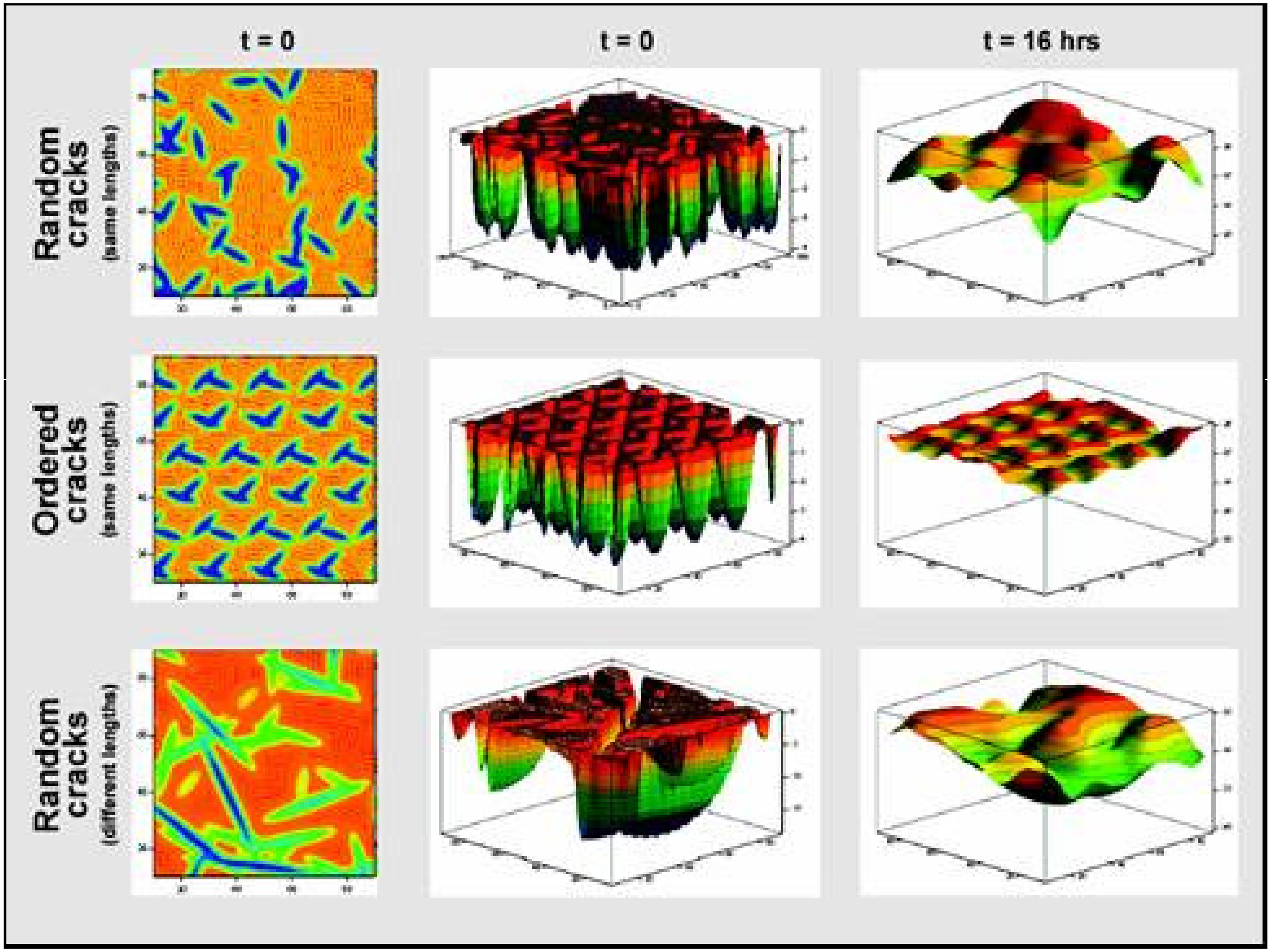

Crack distribution strongly affects etching time needed for crack annihilation

Science & Technology based optical fabrication strategy was implemented to greatly reduced scratch densities

Optical fabrication strategy

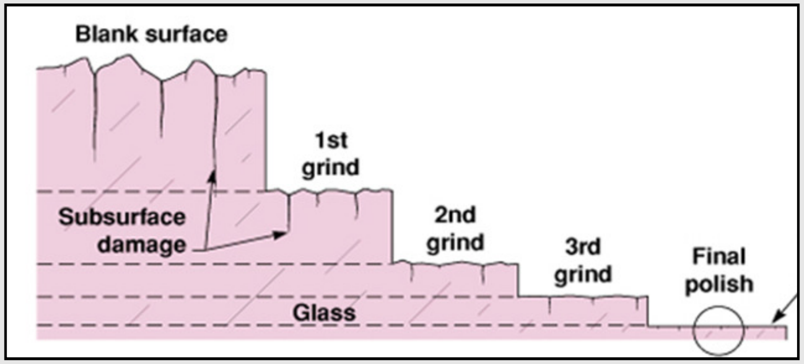

1. Measure the subsurface damage (SSD)
2. Define proper removal
3. Use etching to remove SSD after grinding
4. Ensure handling & cleaning prevents rogue particle contact
5. Remove rogue particles in polishers
6. Use etched scratch inspections
7. Use scratch forensics to identify & mitigate source of scratches

The scratch density has dropped by ~20x in a 10 year period

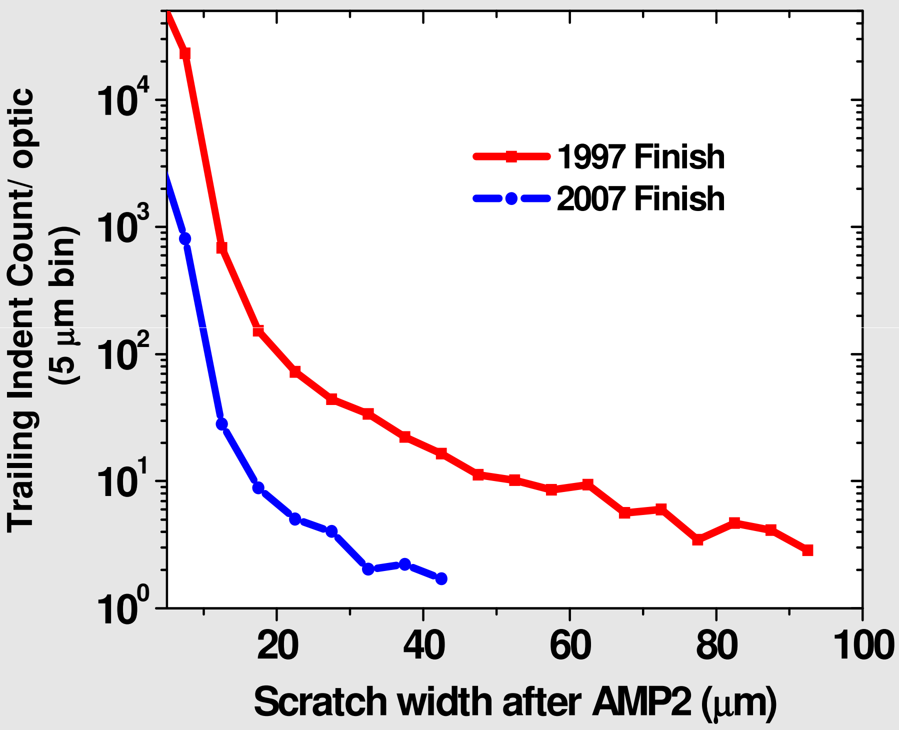

Trailing indent = individual fractures in a scratch

Making intermediate and final polishing more deterministic will allow for making optics faster and cheaper

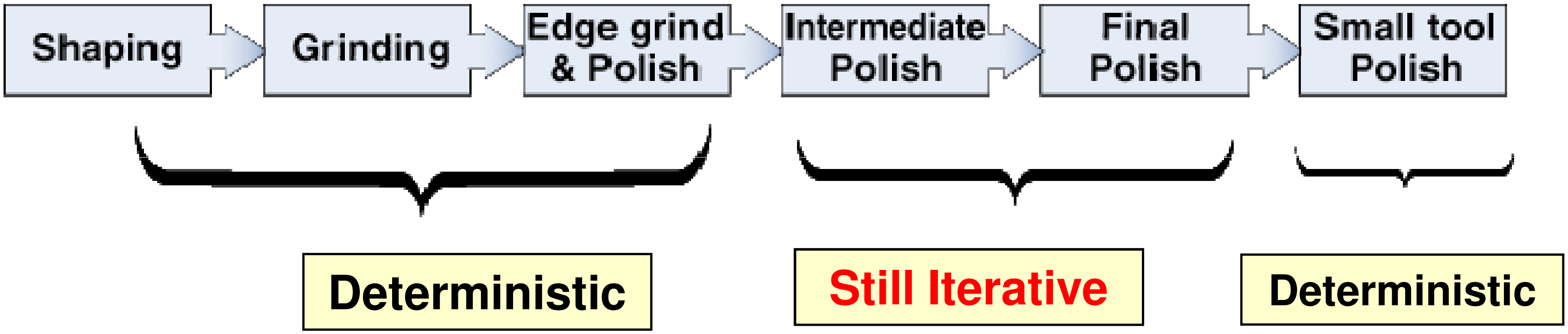

- Involves multiple polishing and metrology iterations
- Time consuming and labor intensive
- Figure not corrected here is performed by small tool

Systematic effort to understand all the phenomena that affect material removal has been conducted

$$\frac{dh}{dt}(x,y,t)=\underbrace{k_p}\,\underbrace{\mu(x,y,t)}\,\underbrace{v_r(x,y,t)}\,\underbrace{s\,(x,y,z,t)}$$

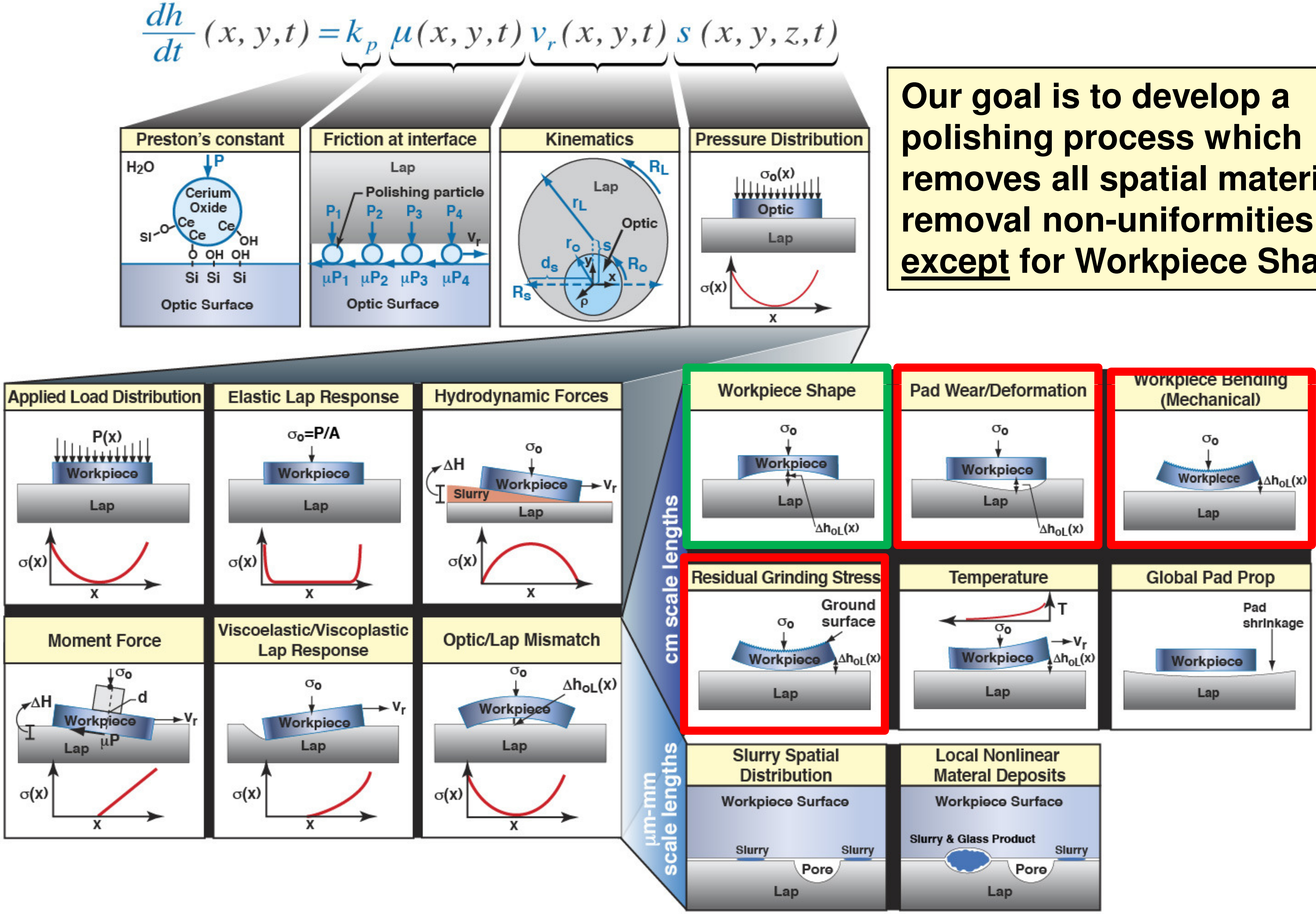

Our goal is to develop a polishing process which removes all spatial material removal non-uniformities <u>except</u> for Workpiece Shape

A novel septum has been designed to counteract non-uniform wear on the pad

Pad wear vs lap radius due to workpiece and engineered septum

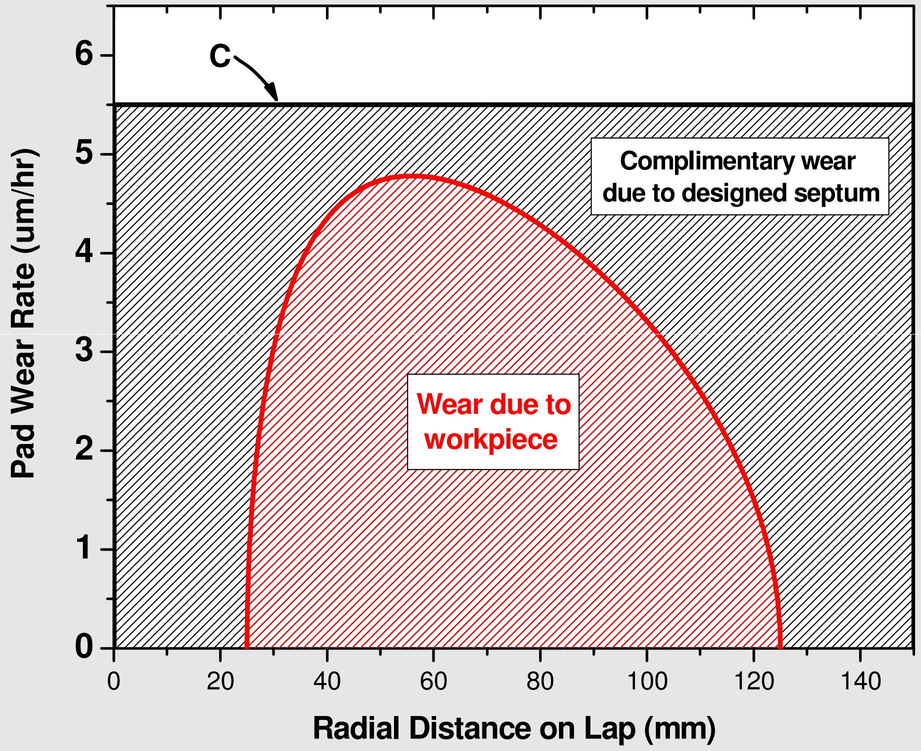

$$\frac{dh_L(r)}{dt} = C = \underbrace{f_o(r)k_L\mu V_{ro}\sigma}_{\text{lap wear due to workpiece}} + \underbrace{f_s(r)k_L\mu V_{rs}\sigma}_{\text{lap wear due to septum}}$$

Determined shape of Septum

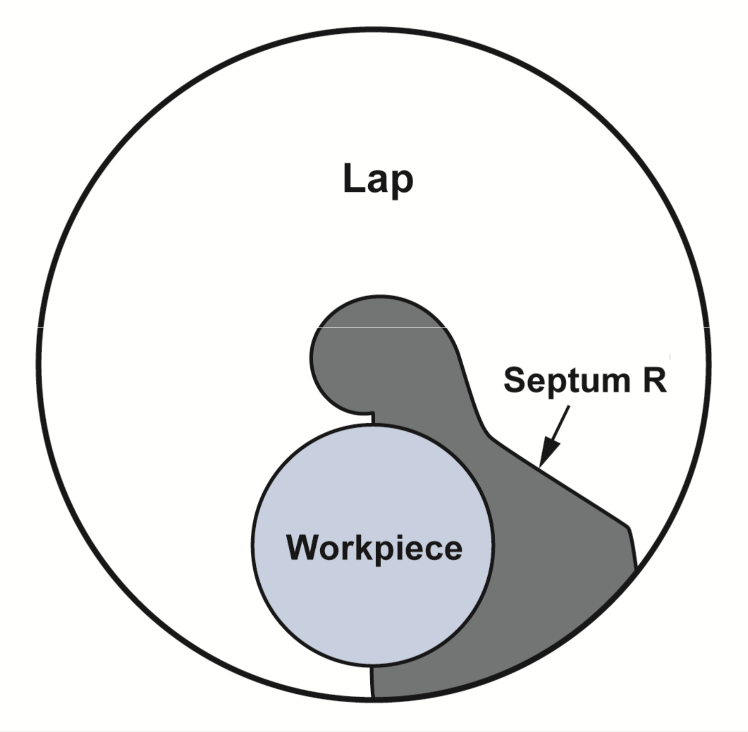

$$w_s(r) = \frac{C - a\sin\left(\frac{x(r)}{r}\right)k_L\mu R_o s\sigma 2r}{k_L\mu R_L r\sigma}$$

T. Suratwala,US Provisional Patent Application 61454893 (Mar 2011)

Chemical etching can effectively remove the residual stress and any complications to workpiece-lap mismatch

Surface Figure of S2 (Initial)

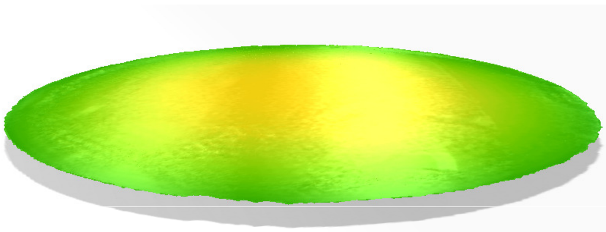

PV$_q$= -1.29 μm

- Polished Fused silica Workpiece (100 mm x 2.2 mm thick)

Surface Figure of S2 (After Grinding S1)

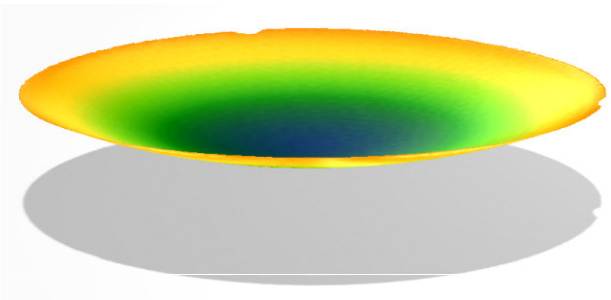

PV$_q$= 3.65 μm

- Grinding S1 puts compressive stress on S1; Hence S2 bends 4.8 μm
- Behavior shown to follow Twyman's Stress effect

$$PV = \frac{3}{4}\frac{P_o(1-\nu)}{E}\left(\frac{D}{t}\right)^2$$

Surface Figure of S2 (After Grinding/Etching*)

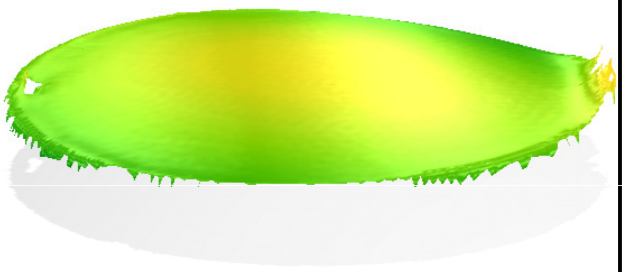

PV$_q$= -1.16μm

- Chemical etching removes residual stress & returns figure to initial state
- Etching after grinding will eliminate residual stress effects & contributions to non-uniform removal

T. Suratwala, IJAGS 3(1) 14-28 (2012)

New Pitch Button Blocking (PBB) process provides low deflections for fused silica and phosphate glass

**100 mm (diam) x 2.2 mm (thick)
Fused Silica PBB**

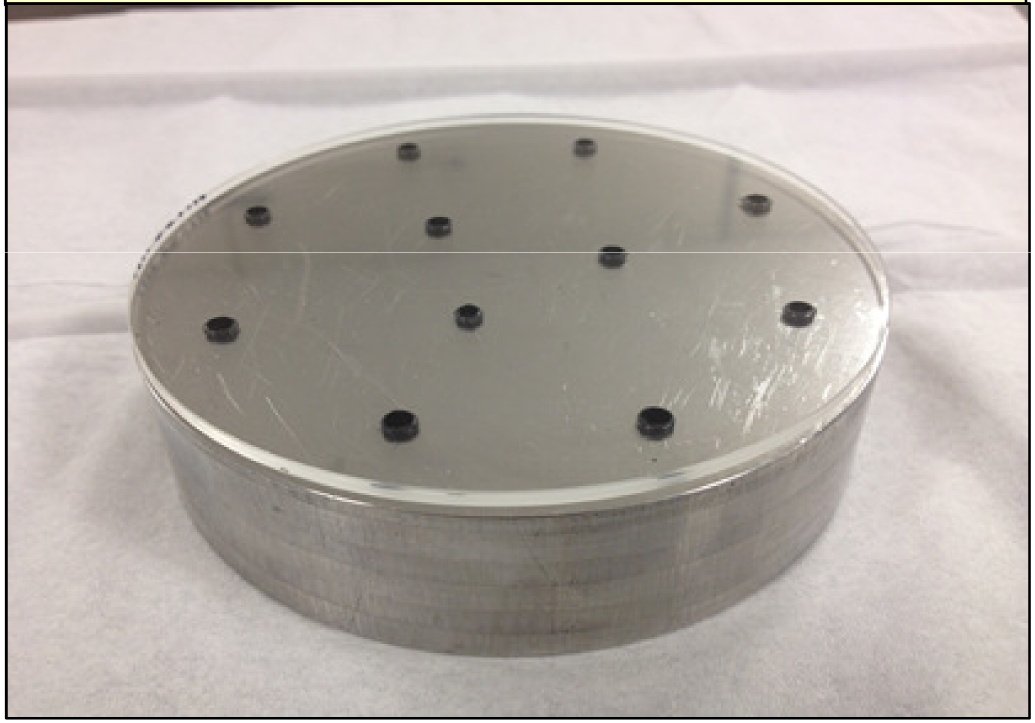

**264 mm (side) x 8 mm (thick)
Fused Silica PBB**

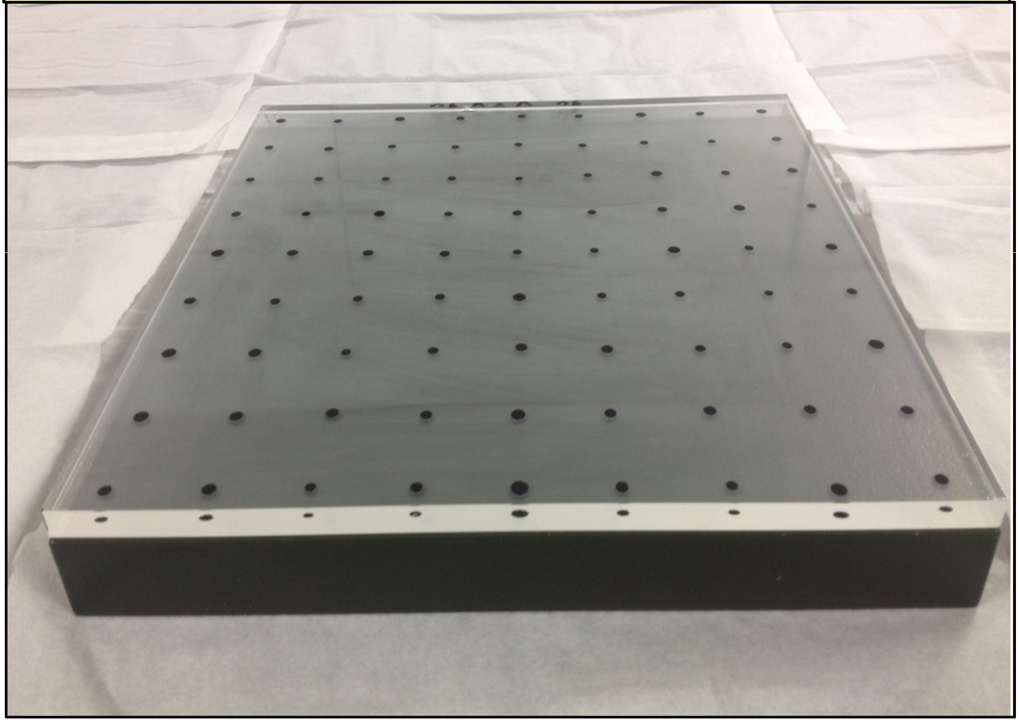

FS	**ΔPV=0.003 μm**
Phosphate	**ΔPV=0.035 μm**

M. Feit, ***Applied Optics*** **51(35) 2012 8350-59**

A thermo-elastic model, with stress relaxation of pitch, can explain PBB behavior

FlexPDE Model for PBB calculates deflection due to thermoelastic deflection

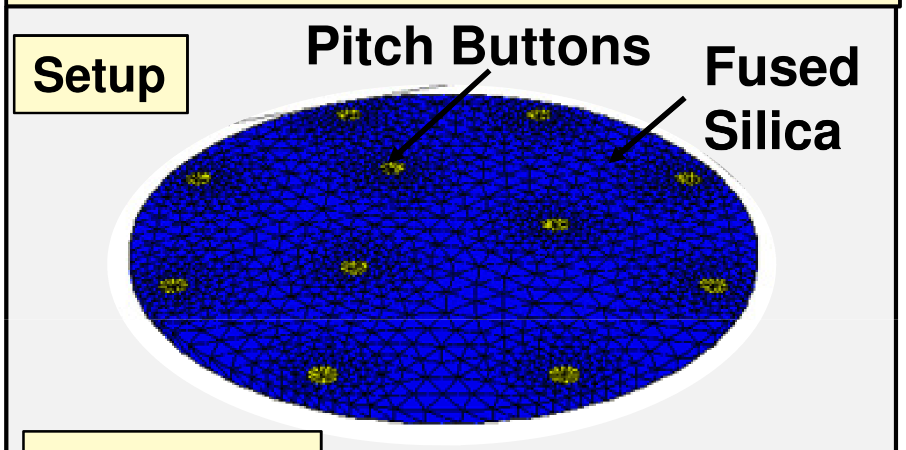

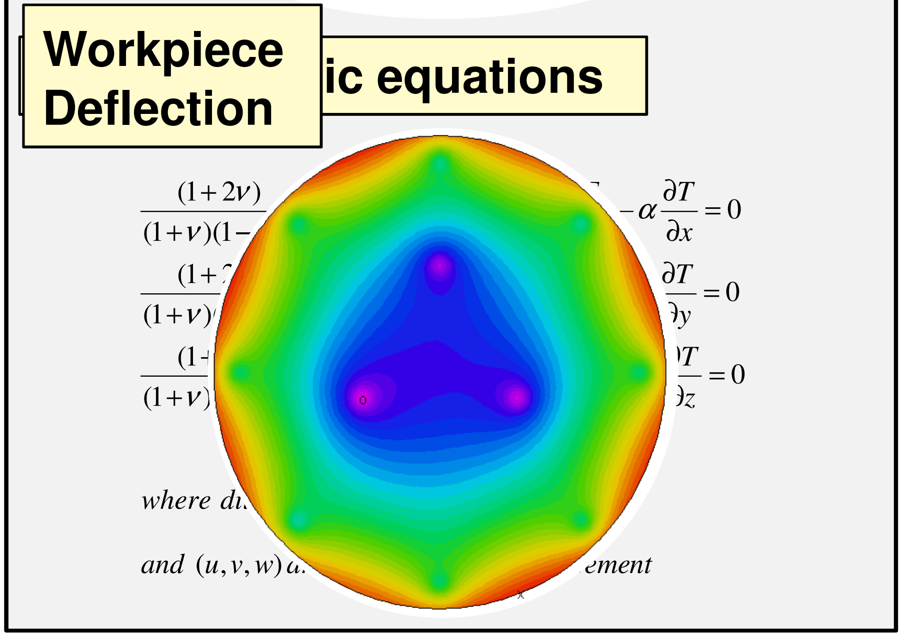

Model vs Experiment: ΔPV as fn of pitch button area fraction

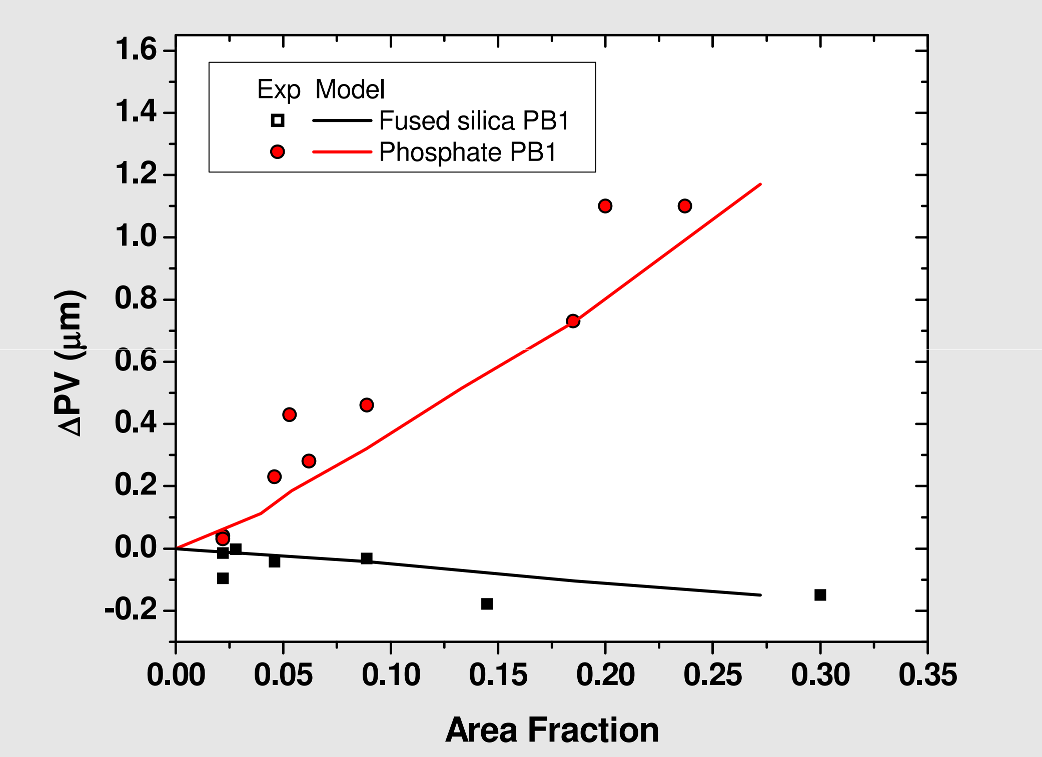

- **Eff. thermal exp. coeff. of pitch to incorporate stress relaxation**
  - **Measured α_{pitch}=37.5 x10^6 K^{-1}**
  - **Used in Model α_{pitch}=2.4 x10^6 K^{-1}**
- **Have established a engineering rules for button design and repeatable process**

M. Feit, *Applied Optics* (Dec. 2012)

The major sources of non-uniform spatial removal been identified and mitigated

Workpiece Surface vs. Polishing Time for Different Configurations

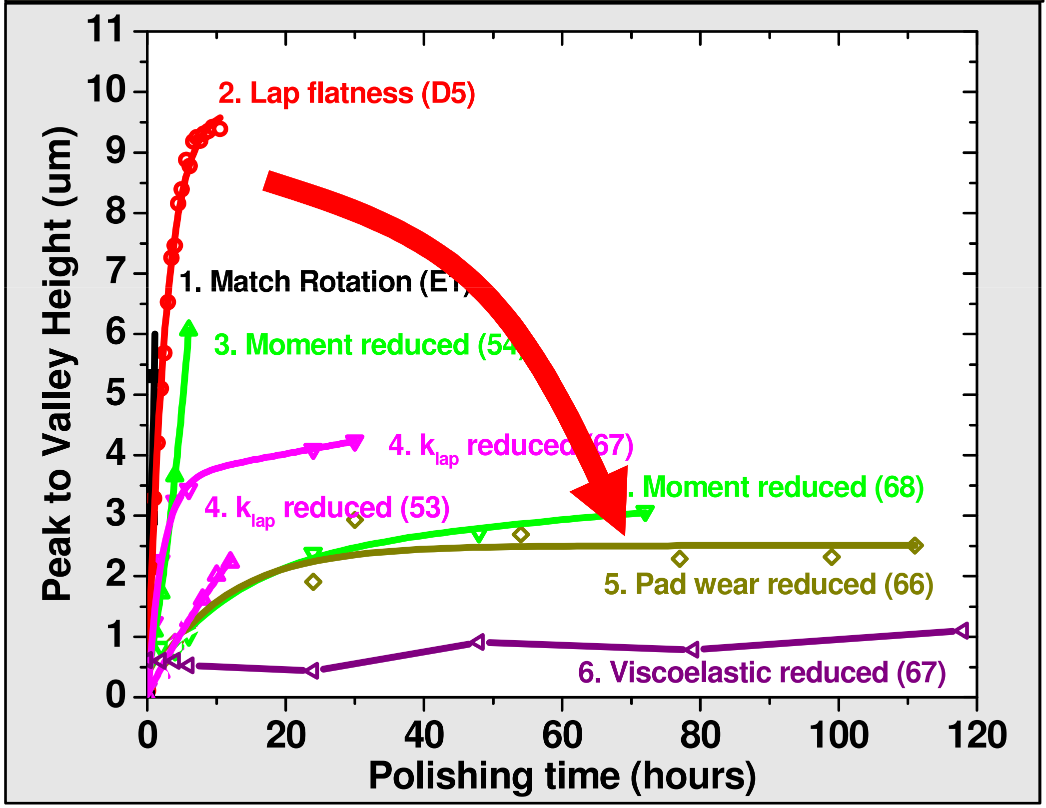

For all polishing runs: r_o=50 mm; r_L=150 mm; s = 75 mm; r_s,d_s=0; P_A=0.3 psi

Polishing Without Uniformity control

Before polish

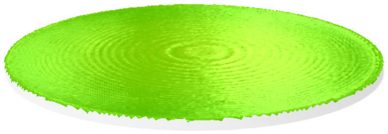

After polish (45 hr)

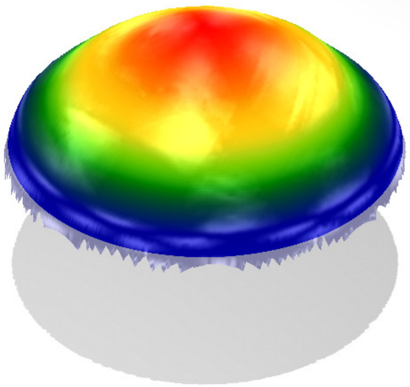

Polishing With Uniformity Control

Before polish

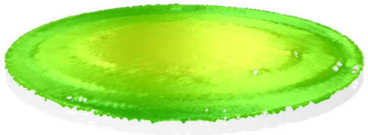

After polish (45 hr)

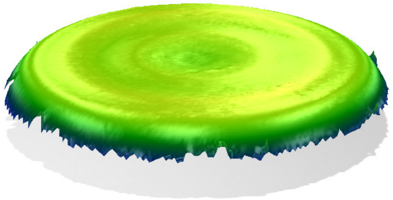

T. Suratwala, IJAGS 3(1) 14-28 (2012)

New Convergent Polishing has been demonstrated on 4”-10” round & square plano glass optics

Surface Convergence on 4” square

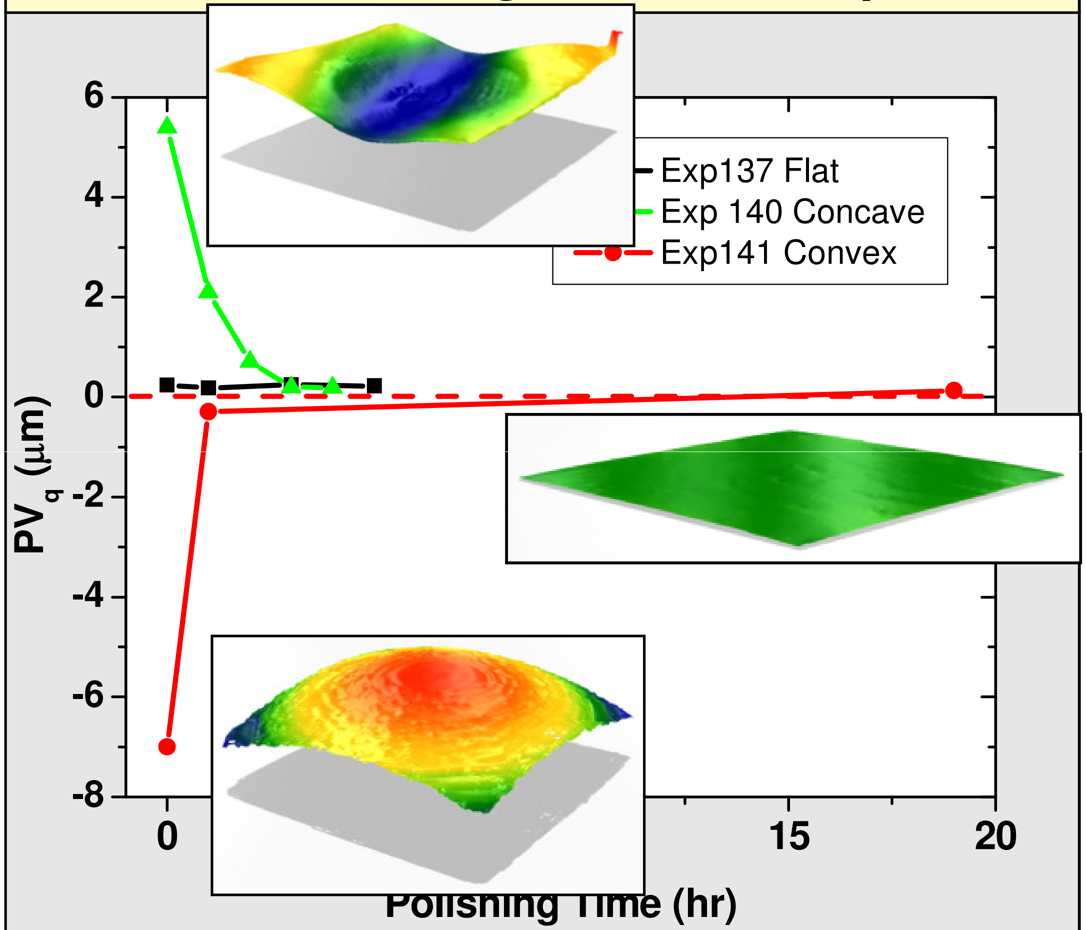

- **Convergence band:**
  PV= 0.18 ± 0.04 µm (~λ/3)

T. Suratwala, IJAGS 3(1) 14-28 (2012)
T. Suratwala , US Patent Application 61454893 (Mar 2011)

The Preston model has been extended to the microscopic scale to describe smaller spatial scale length effects

Macroscopic Material Removal

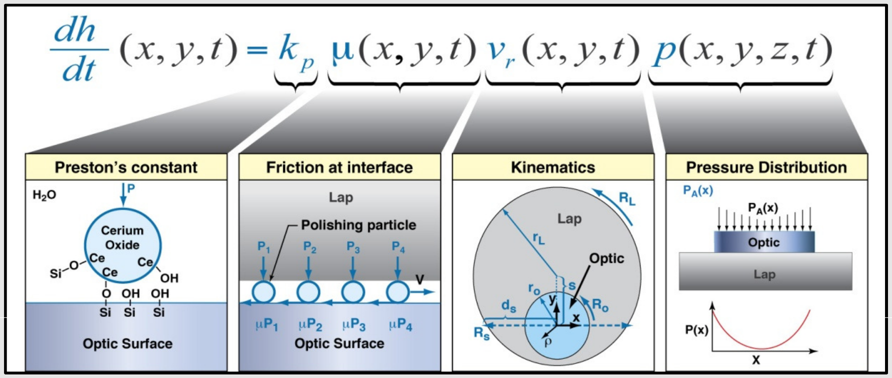

$$\frac{dh}{dt}(x,y,t) = \underbrace{k_p}\ \underbrace{\mu(x,y,t)}\ \underbrace{v_r(x,y,t)}\ \underbrace{p(x,y,z,t)}$$

- Describes removal and surface for scales length > 1 mm
- k_p and μ is macroscopic ensemble values

Microscopic Material Removal

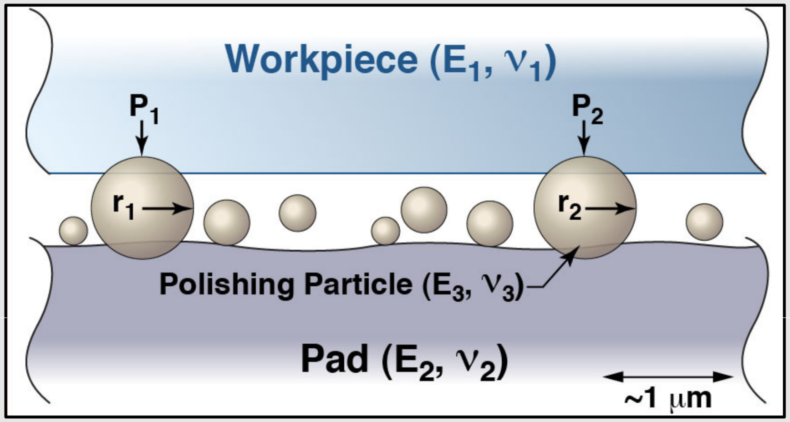

- Describes removal and surface for scales lengths nm to mm
- Hertzian contact zone determines removal area
- Lap topology and particle size dist determine number of contacts
- Ensemble determines macroscopic value of k_p and μ

The slurry's tail end of the distribution strongly correlates with workpiece roughness

Measured particle size distributions of ceria slurries

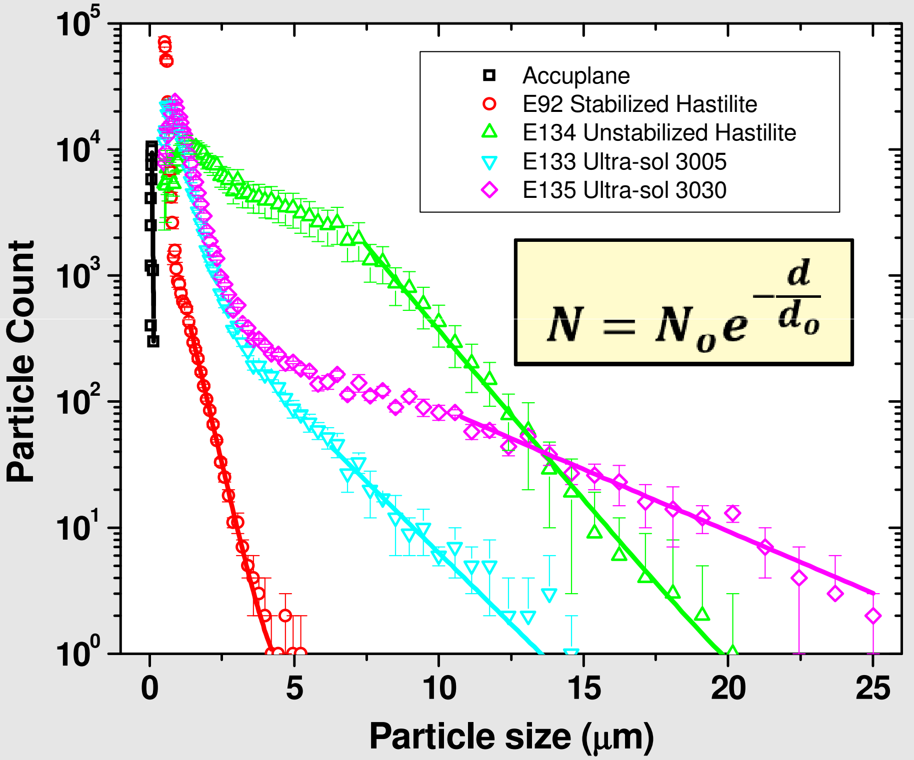

$$N = N_o e^{-\frac{d}{d_o}}$$

The tail end of each slurry can be fit to single exponential distribution

Exponent constant in PSD of slurry vs RMS roughness of polished surface

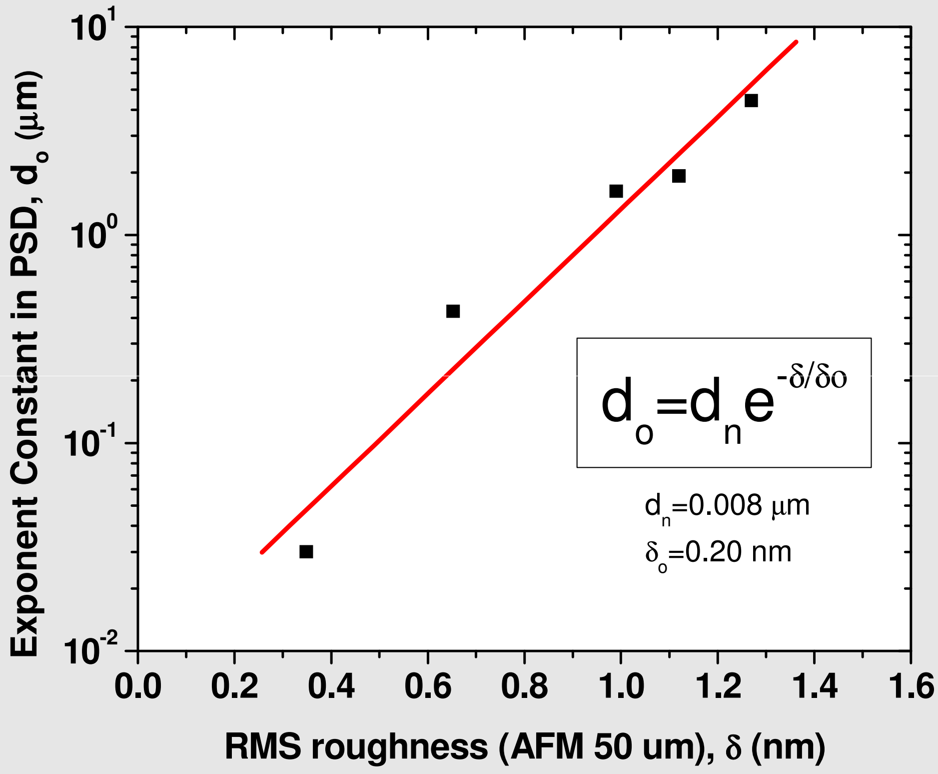

$$d_o = d_n e^{-\delta/\delta o}$$

d_n=0.008 µm

δ_o=0.20 nm

The slope of the slurry's particle size distribution quantitatively scales with the rms roughness

Stresses the need to get slurry PSD with small d_o to get low roughness surface; Mean particle size is not as important!

Single pass of ceria particle removes ~1 nm of material (~7 Si-O units)

AFM Image (2 um x 2um) of Sample 4

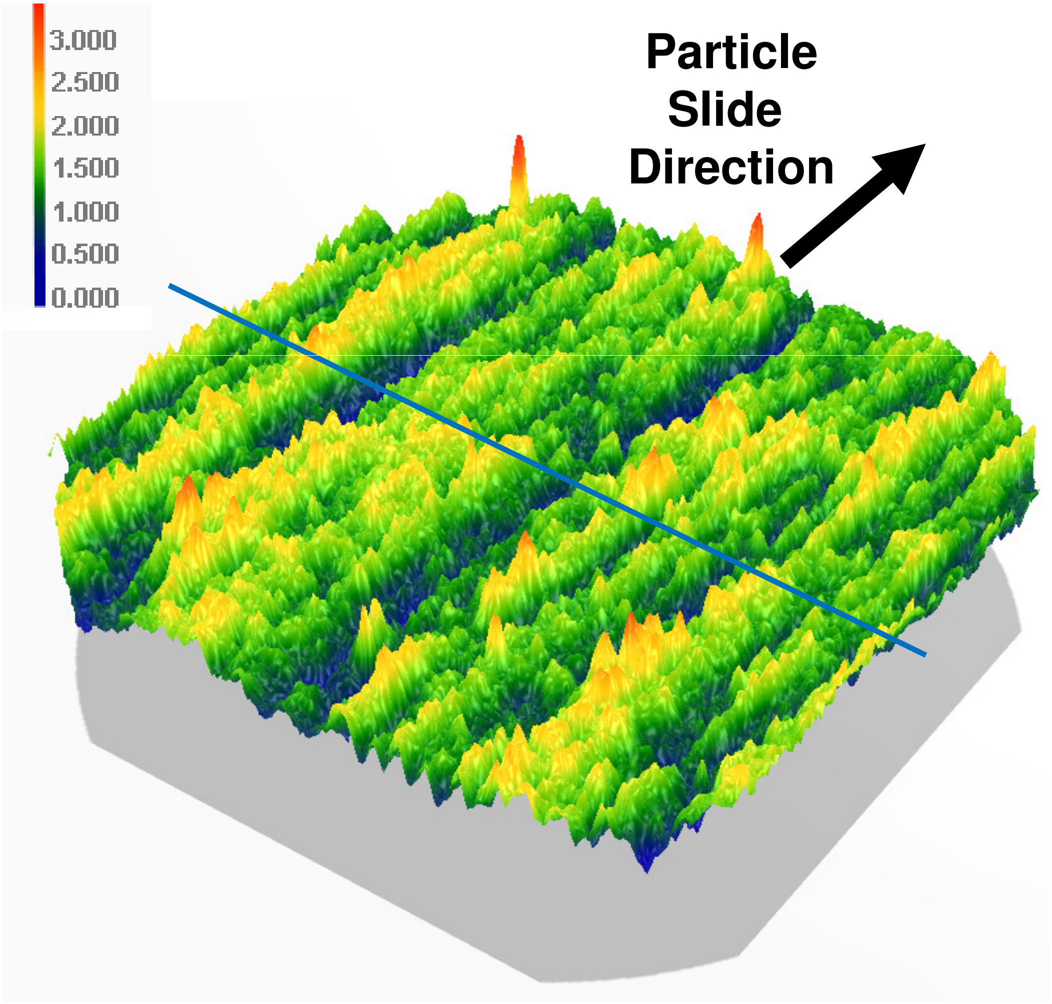

Lineout of AFM Perp. to slide particle slide direction

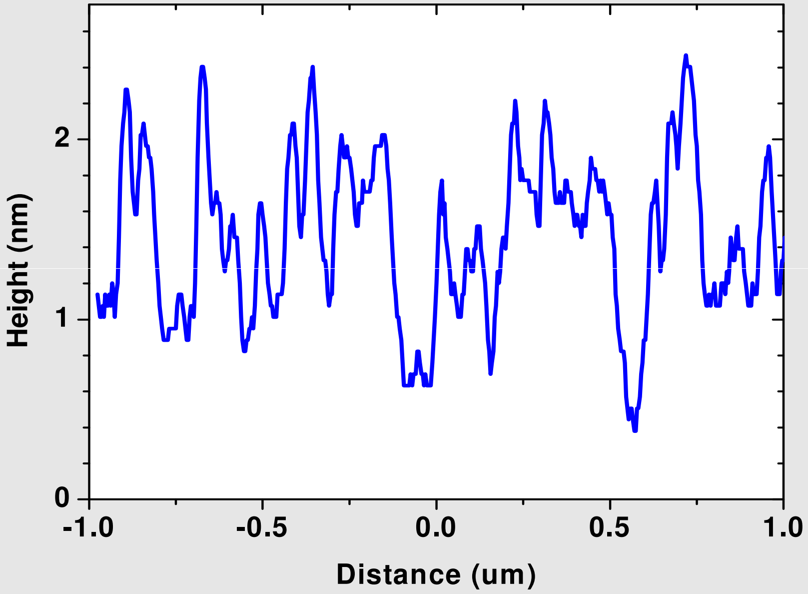

Using a single set of parameters, polished surfaces have been simulated over multiple spatial scale lengths using different slurry particle size distributions

11/23/12

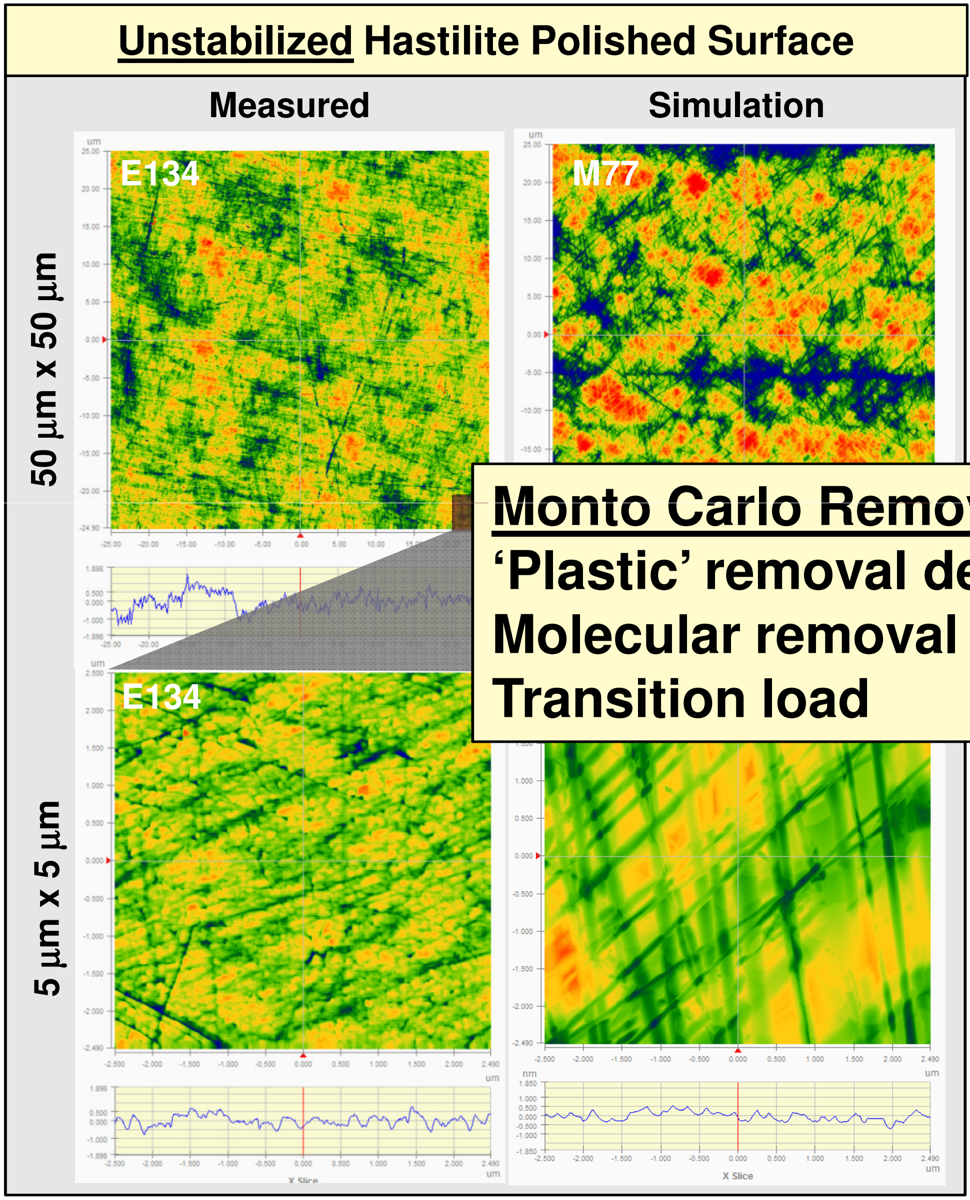
Unstabilized Hastilite Polished Surface

Monto Carlo Removal Parameters

‘Plastic’ removal depth $d_r = 1$ nm

Molecular removal depth $d_m = 0.04$ nm

Transition load $P_{crit} = 4\times10^{-5}$ N

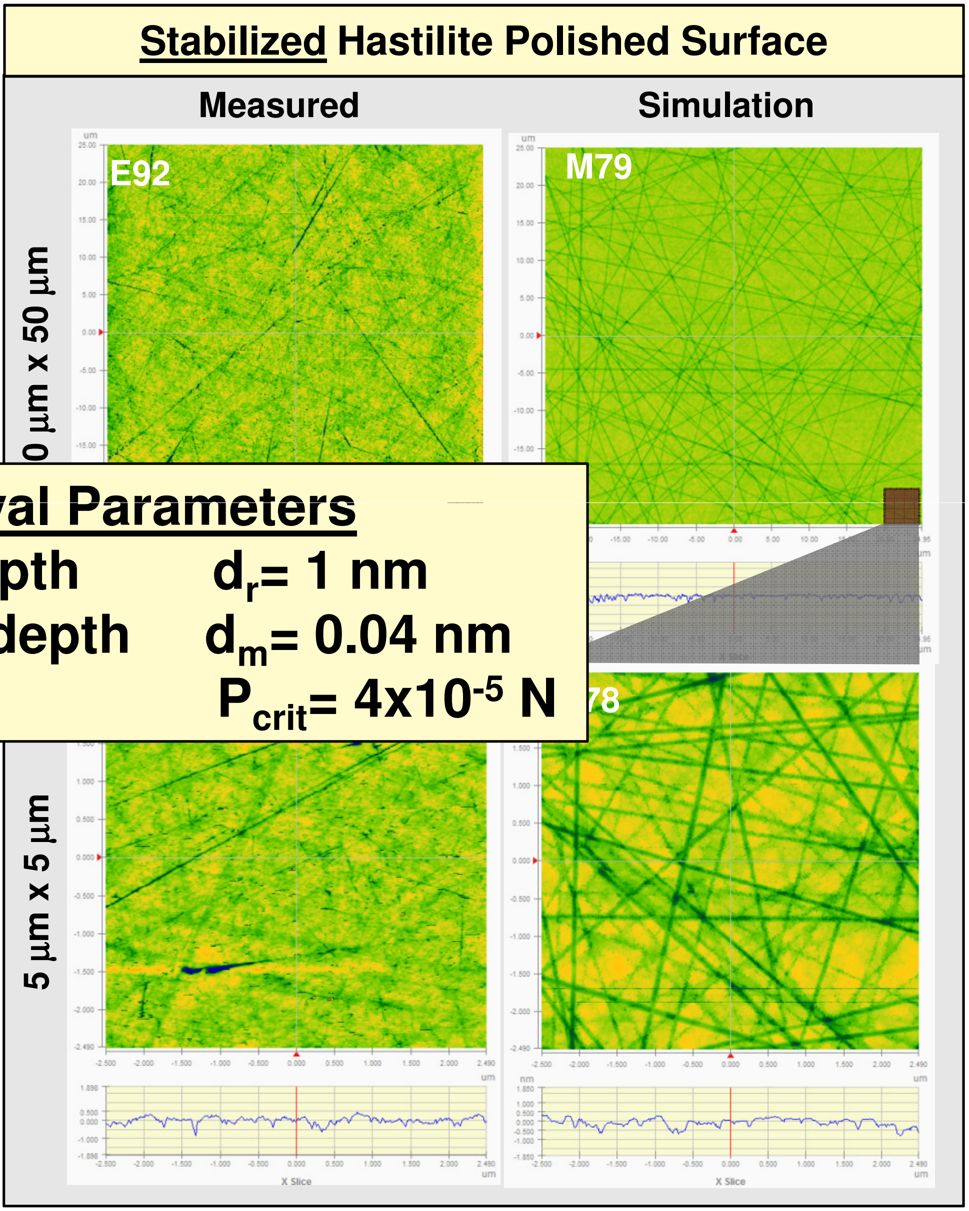
Stabilized Hastilite Polished Surface

M76-79 Zernikes removed Only

dr=1nm; mol removal=0.04 nm

Our S&T has focused on understanding surface interactions on glass surfaces during fabrication, post processing and laser operation

	1. Optical Fabrication	2. Post Processing & Coatings	3. Laser Operation
Current Efforts	• Sub-surface damage management • Forensics of surface fractures • Fundamentals of material removal • Technology of full aperture & small tool optical finishing • Low cost, precursor-free finishing techniques	• Development of chemical/thermal-based flaw/damage mitigation • Development of laser-based flaw/damage mitigation • Laser interference gratings development	• Mechanism of initiation & growth (precursors & modulation) • Precursor isolation & identification • Quantitative understanding initiation & growth behavior • Understanding solarization effects • Understanding modulation effects
Future Challenges	• Toward deterministic finishing (away from artisan, iterative finishing) • Science of finishing continued (microscopic, molecular, & chemical interactions) • Development of new finishing techniques		• Higher fluence precursor identification & mitigation • Understand multi-pulse surface & radiation effects • Understand/mitigating debris-induced damage • Understand damage mechanisms on other glass optics (including coatings) • Development of new glass optical materials (e.g., high fluence optical filters)

Optimization of etching processes have led to large increases in the damage resistance of scratches

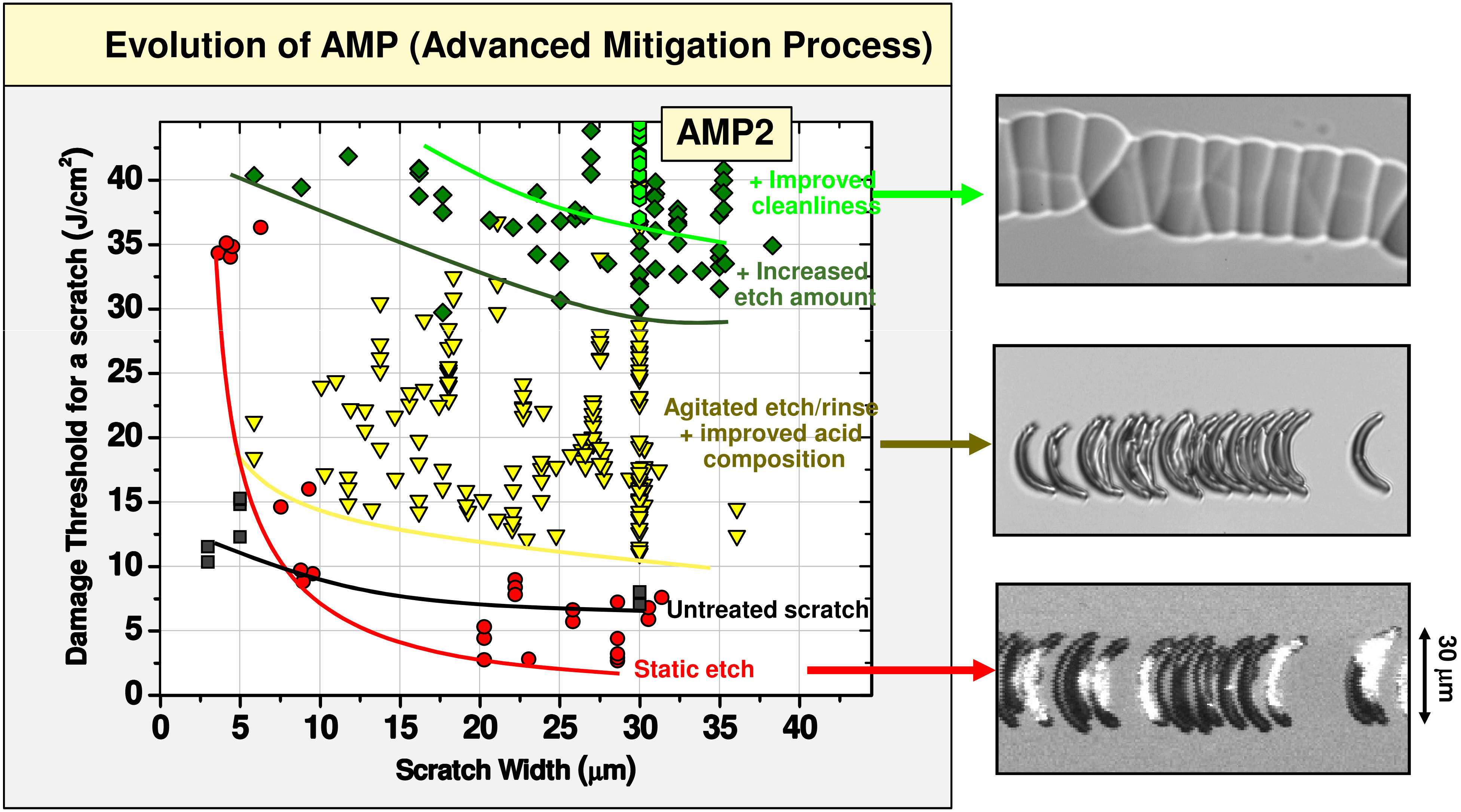

Evolution of AMP (Advanced Mitigation Process)

T. Suratwala, et. al. *J. Am. Cer. Soc.* 94 (2) (2010) 416-428; P. Miller, et. al. *US Patent 8,313,662* (11/20/12)

Using a mass transport model, process has been optimized to minimize reaction product concentration left in the crack

Calculated SiF_6^{2-} concentration during AMP Process

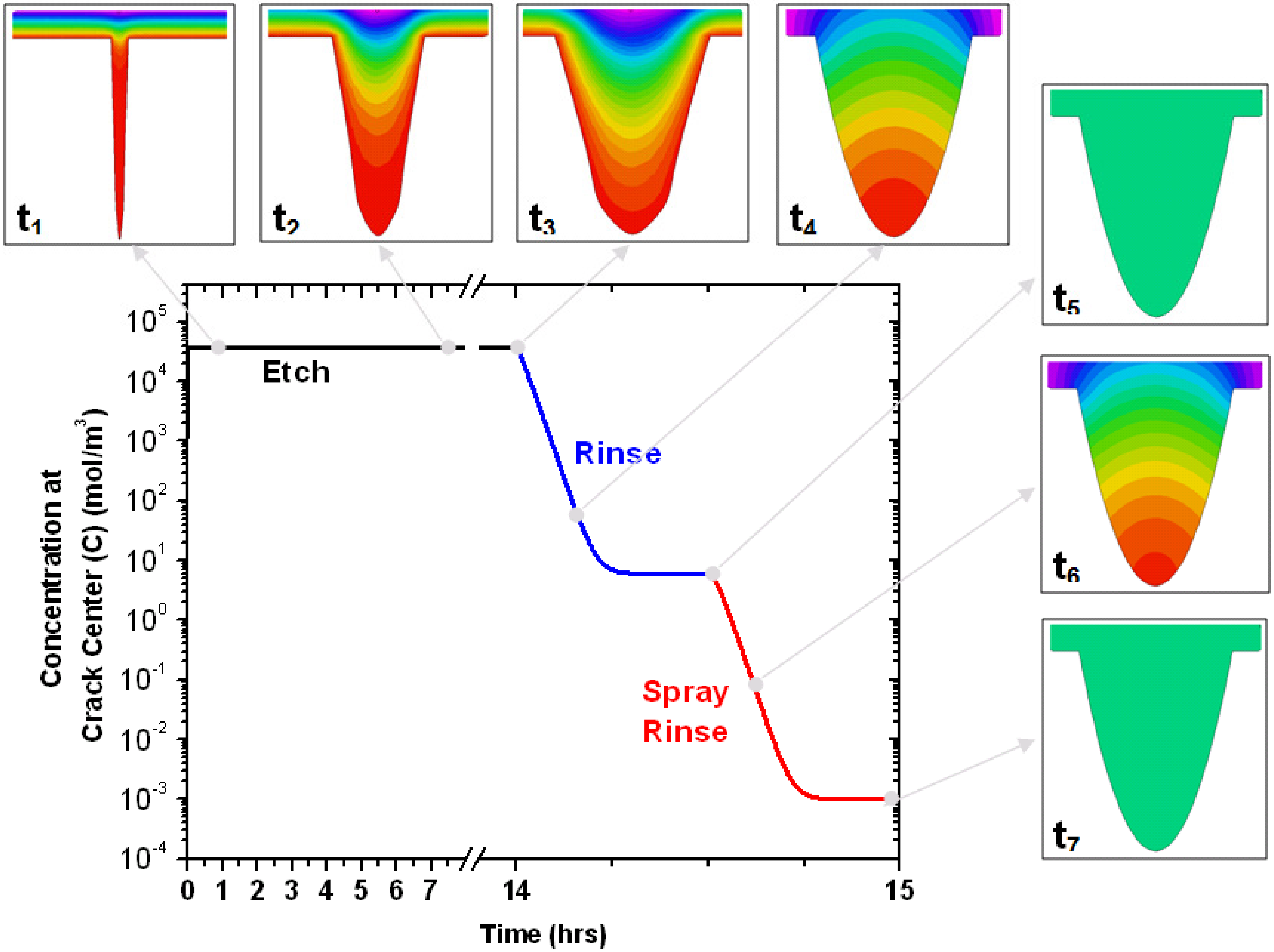

Using AMP2, scratches as a damage precursor in NIF have been eliminated

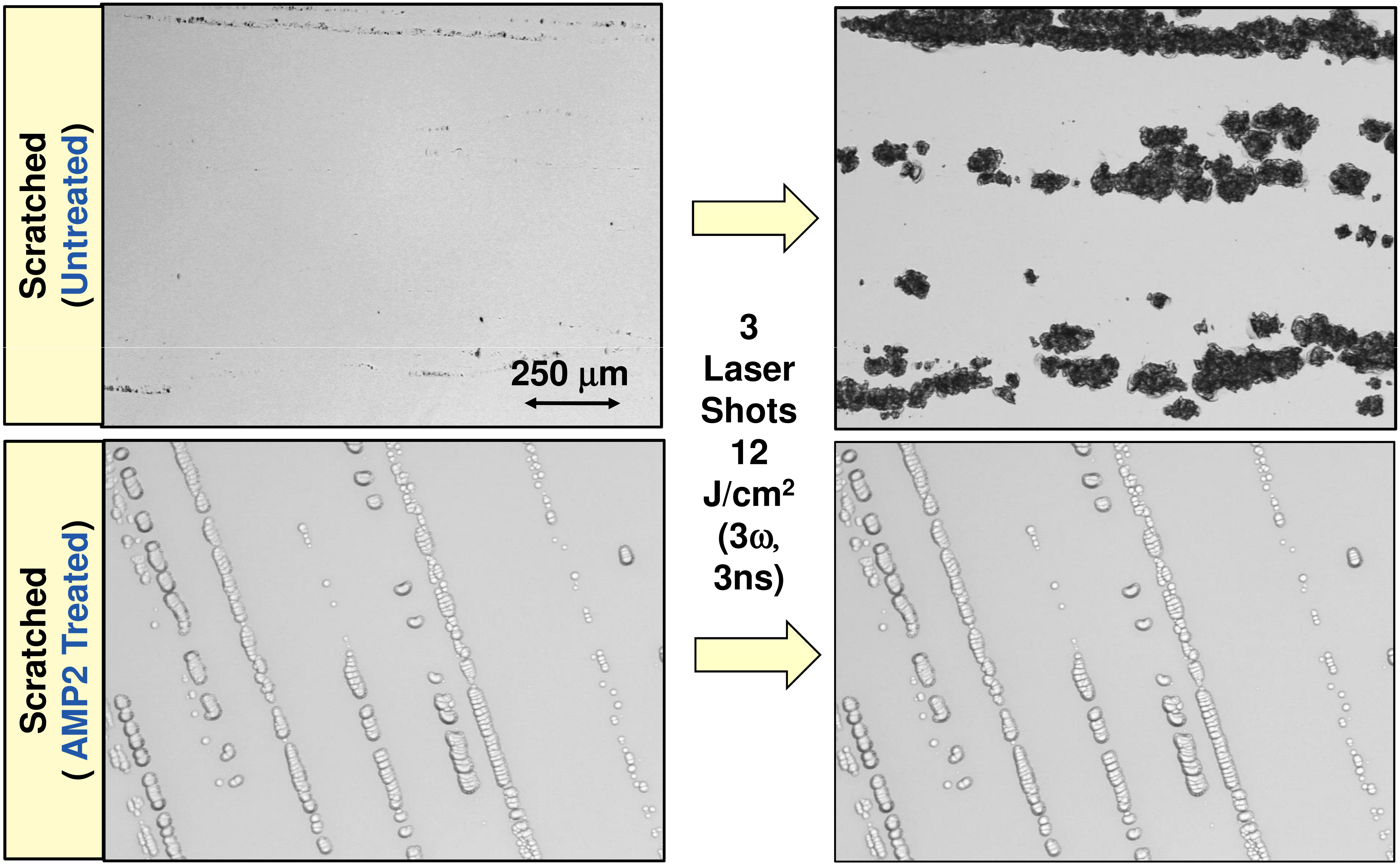

Scratched (Untreated)

Scratched (AMP2 Treated)

3 Laser Shots 12 J/cm^2 (3ω, 3ns)

AMP2 in production

Flaws on fused silica are mitigated with a small-beam CO_2 laser operating at 10.6-μm

Rapid Ablation Mitigation (RAM) Protocol

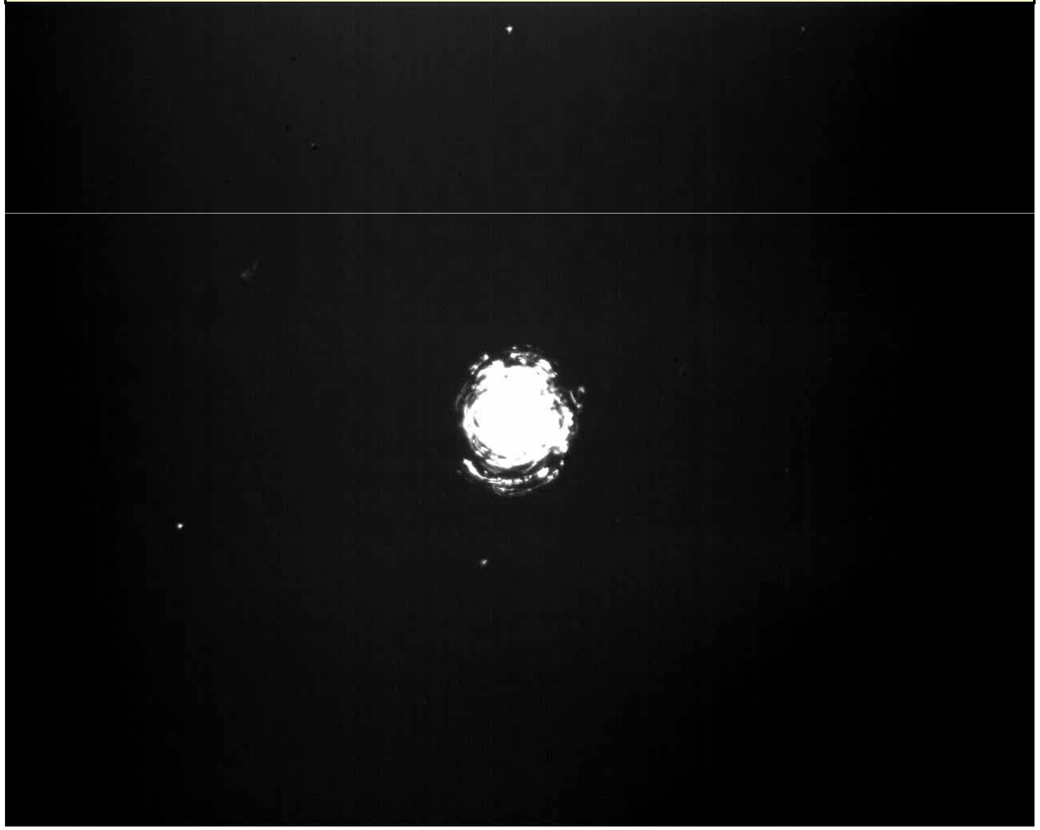

- Utilizes rapid scanning of tightly-focused high-power CO_2 laser pulses to remove flaws up to ~0.5 mm diameter
  - — Precise shape control
  - — Fairly wide process margin
  - — Scalable
  - — Damage robust
- The cone is the only shape identified that does not lead to downstream intensification

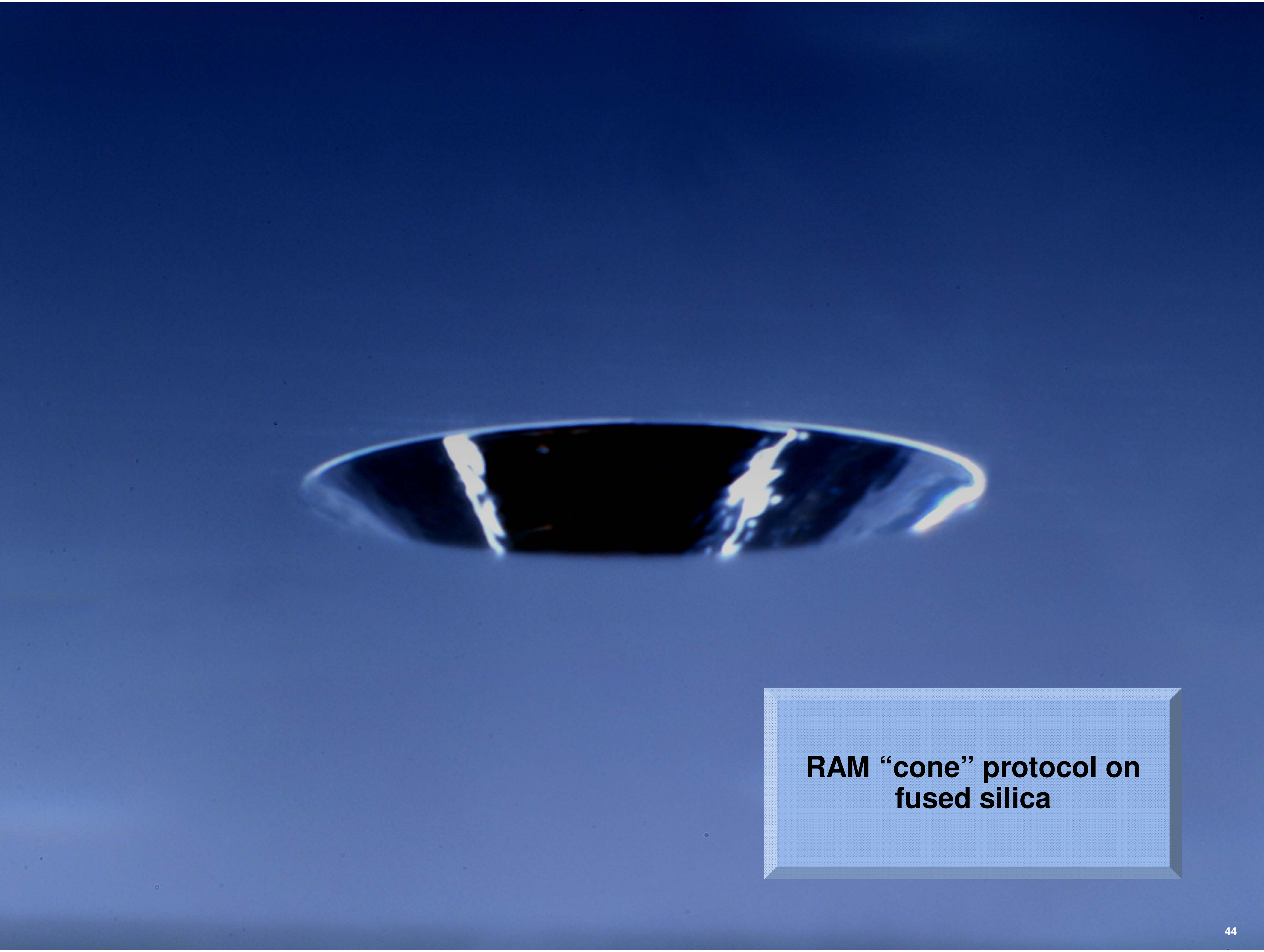

RAM “cone” protocol on fused silica

Successful optics damage mitigation can only be achieved through careful balance of coupled, sometimes competing effects

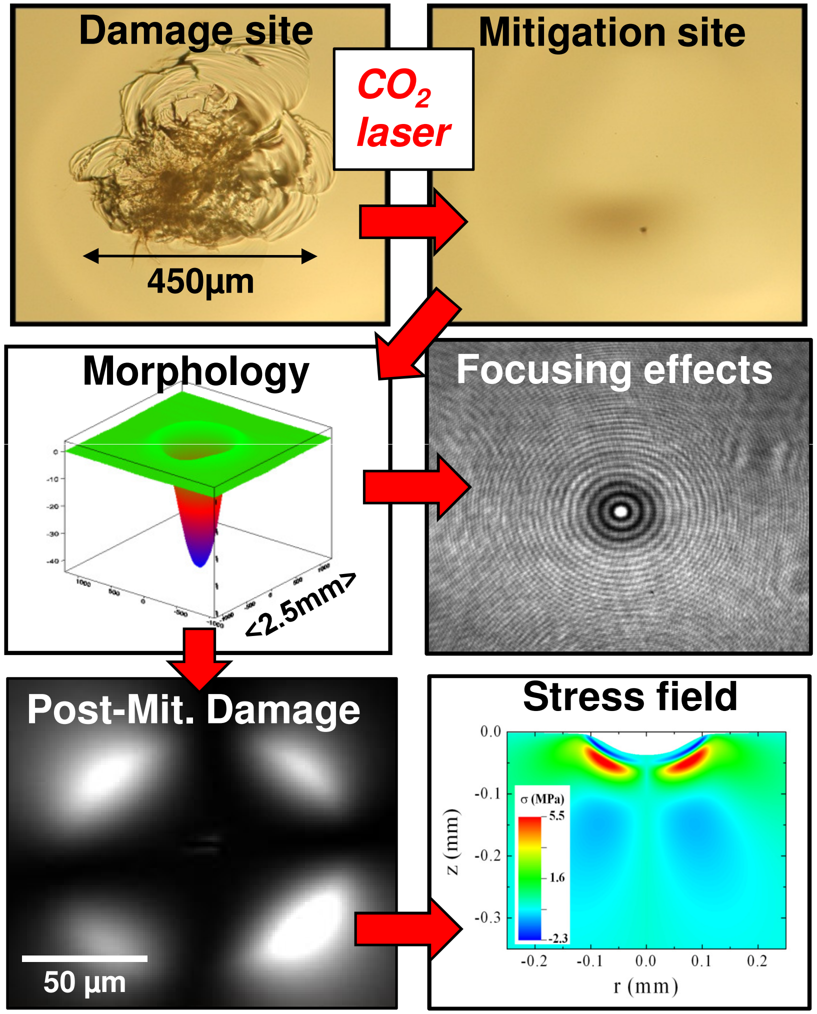

- **<u>UV damage threshold</u>**
  - Remove or re-flow damaged material
  - Free of damage-prone re-deposit
- **<u>Light propagation</u>**
  - Resulting morphology that does not intensify/focus UV light
- **<u>Residual stress & densification</u>**
  - Stress below critical fracture limit
  - Minimally-extended densification

Our S&T has focused on understanding surface interactions on glass surfaces during fabrication, post processing and laser operation

	1. Optical Fabrication	2. Post Processing & Coatings	3. Laser Operation
Current Efforts	• Sub-surface damage management • Forensics of surface fractures • Fundamentals of material removal • Technology of full aperture & small tool optical finishing • Low cost, precursor-free finishing techniques	• Development of chemical/thermal-based flaw/damage mitigation • Development of laser-based flaw/damage mitigation • Laser interference gratings development	• Mechanism of initiation & growth (precursors & modulation) • Precursor isolation & identification • Quantitative understanding initiation & growth behavior • Understanding solarization effects • Understanding modulation effects
Future Challenges	• Toward deterministic finishing (away from artisan, iterative finishing) • Science of finishing continued (microscopic, molecular, & chemical interactions) • Development of new finishing techniques	• Development of new chemical & laser mitigations strategies (e.g., for high fluence precursors, damage sites, conditioning) • Development of higher fluence multi-layer dielectric coatings • Development of stable, high fluence AR coatings	• Higher fluence precursor identification & mitigation • Understand multi-pulse surface & radiation effects • Understand/mitigating debris-induced damage • Understand damage mechanisms on other glass optics (including coatings) • Development of new glass optical materials (e.g., high fluence optical filters)

The optics S&T effort is a multi-disciplinary, multi-team effort

PLS

- D. Aberg
- S. Baxamusa
- J. Bude
- S. Demos
- R. Dylla Spears
- P. Ehrmann
- P. Erhart
- S. Elhadj
- J. Fair
- G. Gilmer
- T. Laurence
- M. Johnson
- M. Matthews
- J. Menapace
- P. Miller
- M. Monticelli
- R. Negres
- R. Qiu
- R. Raman
- B. Sadigh
- K. Schaffers
- E. Schwegler
- R. Steele
- C. Stolz
- T. Suratwala
- L. Wong
- J. Wolfe

NIF

- J. Adams
- I. Bass
- W. Carr
- D. Cross
- R. Desjardin
- M. Feit
- G. Guss
- Z. Liao
- K. Manes
- M. Norton
- M. Nostrand
- M. Spaeth
- T. Weiland & the OSL Team
- P. Wegner
- C. Widmayer
- S. Yang

ENG

- R. Vignes
- J. Stolken

+ Production Facilities (Optic Mitigation Factory, Optics Processing Lab)
+ Engineering Group (Design & Fabrication)
+ Metrology and Coordination Group

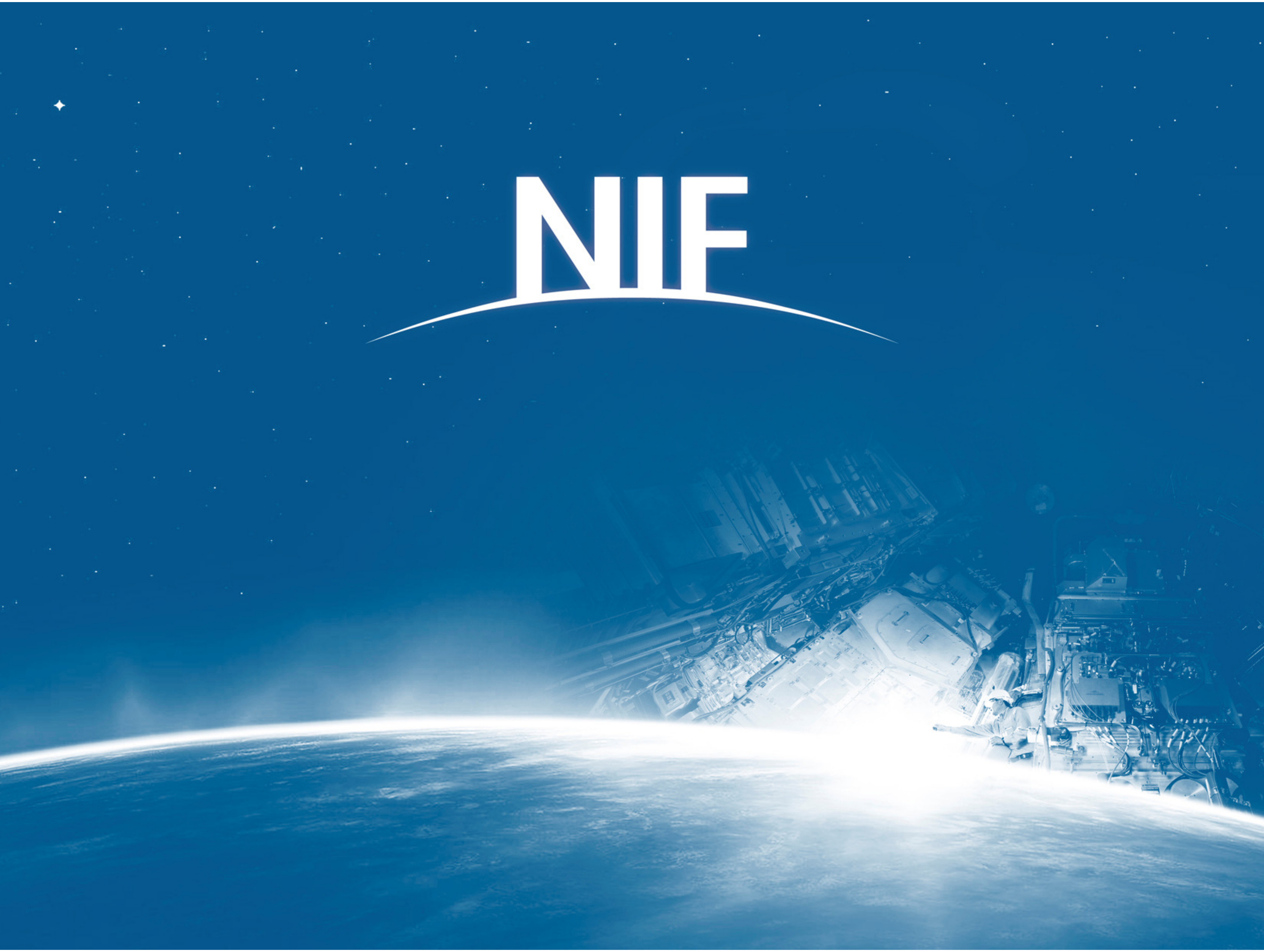
NIF

S&T effort also will focus on developing new high fluence optical filters

Target Performance

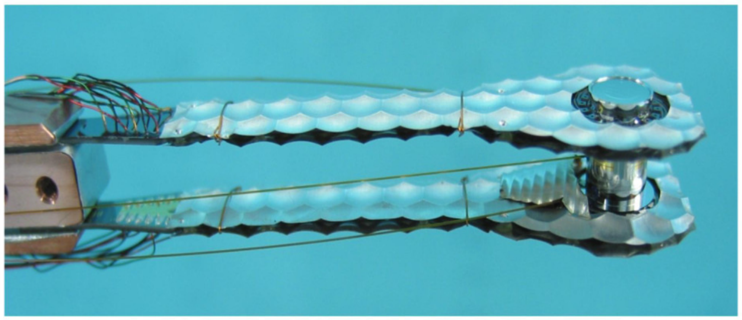

Optic Lifetime

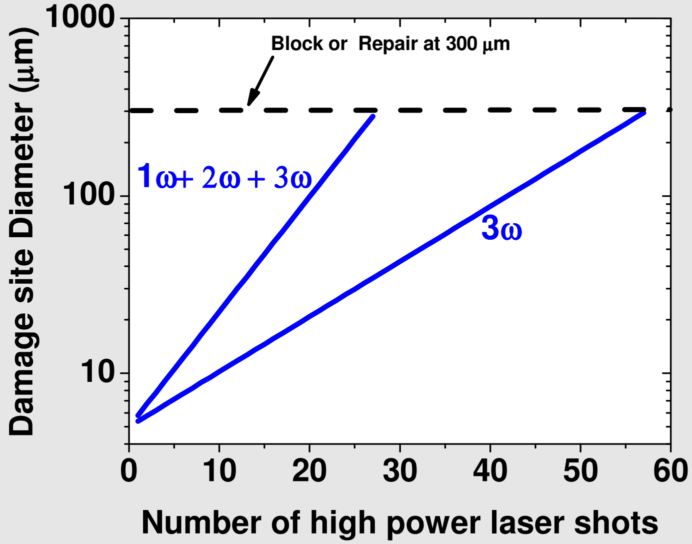

Unconverted laser light degrades target performance and optic lifetime

Example: Red Blocker: Cu^{2+} in glass

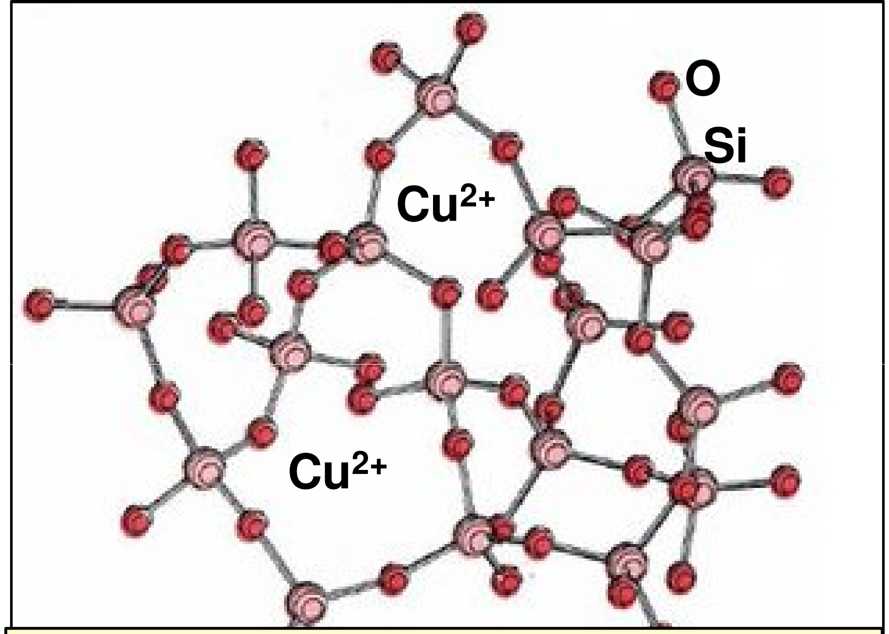

Challenge is to control oxidation state and spectral shifting of absorbing ion within a high fluence resistance glass or liquid host

Collaboration with D. Brow; U. of Missouri

The AF model has also been validated on actual damage sites using tailored laser pulses and comparing to the measured damage core size

Experiment: Create damage initiation sites using tailored pulses

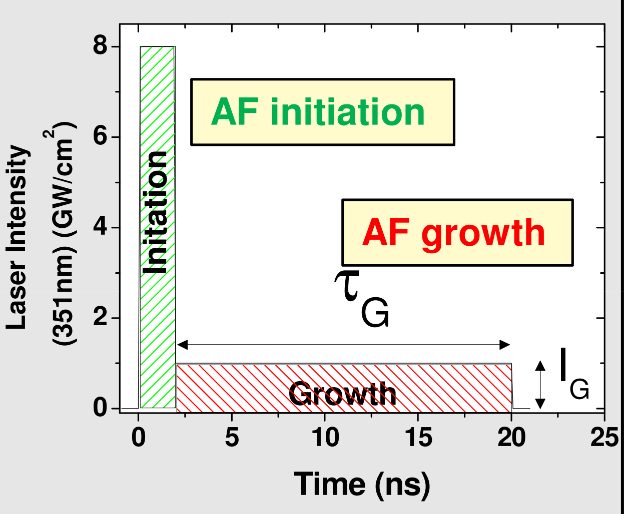

- **Initiation pulse** creates reproducible 2 μm damage sites
- **Growth pulse** drives AF, creates larger molten cores

Results: SEM Micrographs of grown cores

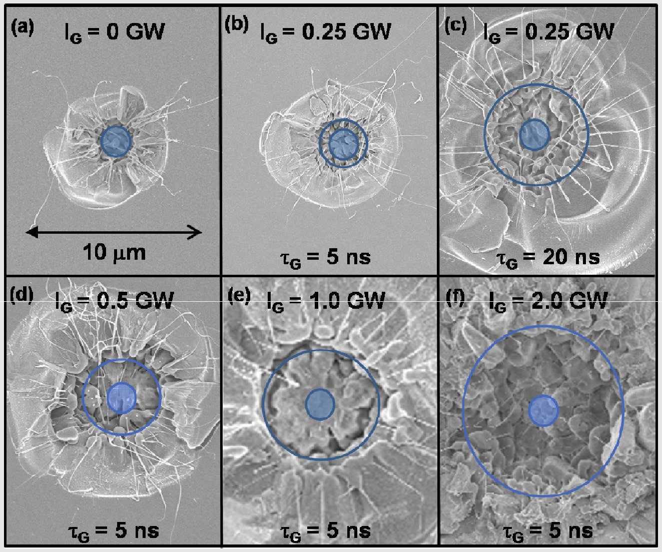

- Outer blue circle indicates the core size for varying growth pulses
- AF velocity determined from change in core size

Model Comparison: AF velocity vs. Laser

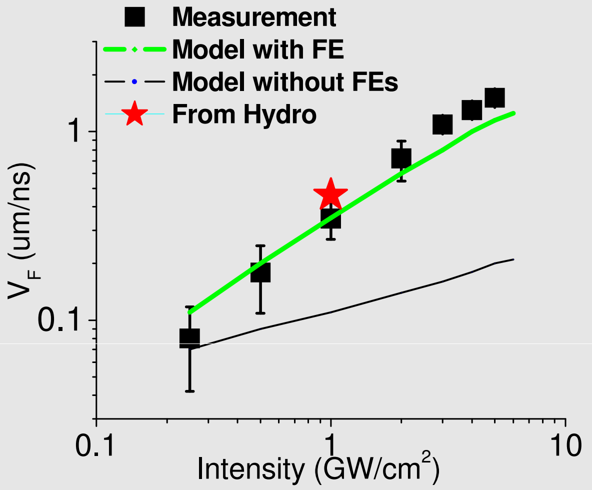

- Modeled V_F from full 1D energy transport sim. and 3D hydro sim.
- Gives key insight into the damage process and the properties of silica under extreme conditions

W. Carr, J. Bude, P. DeMange, PRB 82, 184304 (2010)

There are numerous mechanical, structural and chemical effect on the glass surface during grinding and polishing

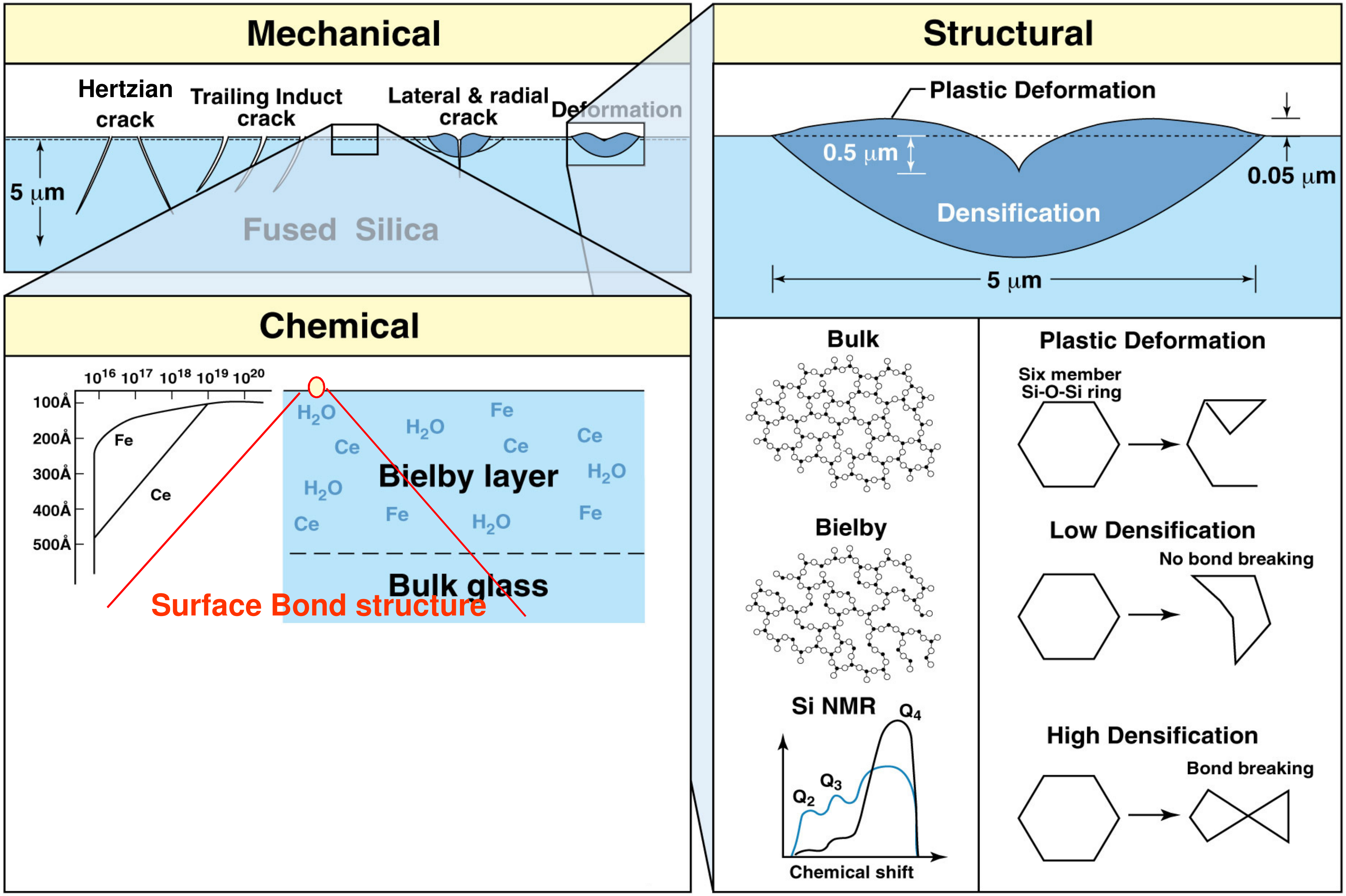

NIF-0307-13436-Lay
16TIS/mfm

There are five major areas of effort that have aided in managing sub-surface fractures

GRINDING

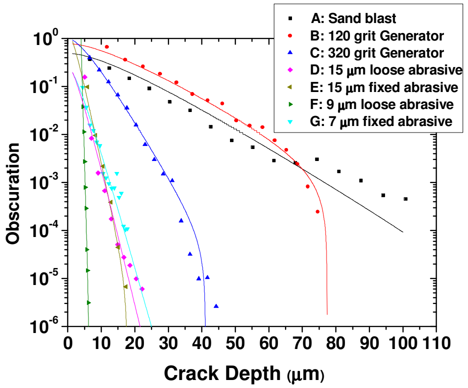

1. Developed fracture mechanics understanding of sub-surface fracture distributions

POLISHING

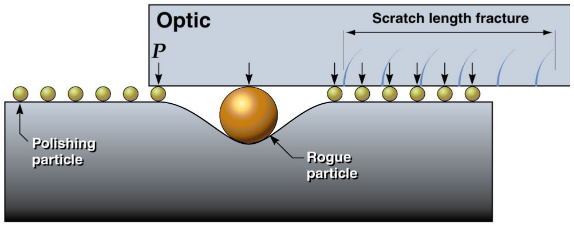

2. Identified/characterized behavior of rogue particles causing sub-surface fractures

CHEMICAL ETCHING

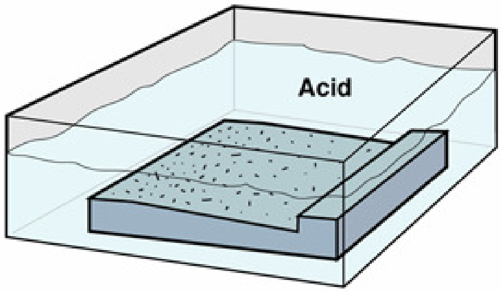

3. Established techniques using etching to reveal and remove subsurface fractures

SCRATCH FORENSICS

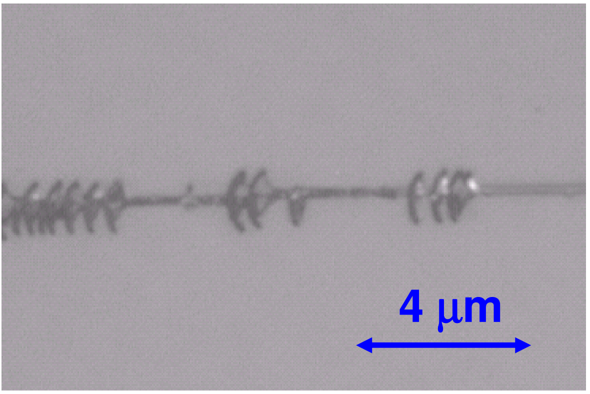

4. Developed quantitative rules for post-diagnosis of cause of surface fractures

LASER DAMAGE

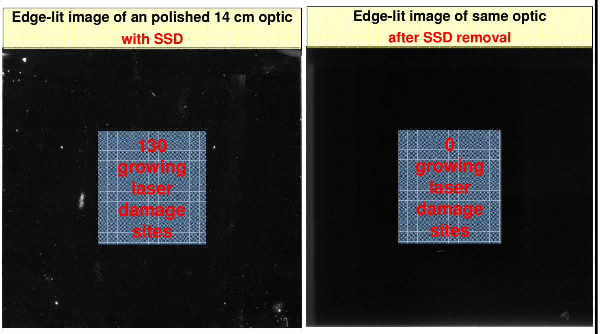
Edge-lit image of an polished 14 cm optic with SSD

Edge-lit image of same optic after SSD removal

5. Showed link between sub-surface fracture removal & improved laser resistance

All of the above have been used to optimize vendor processes to manage sub-surface fractures and to minimize impact of rogue particles

2D mass transport model for SiF_6^{2-} out of a crack during AMP process has been developed

Schematic of 2D Mass transport model

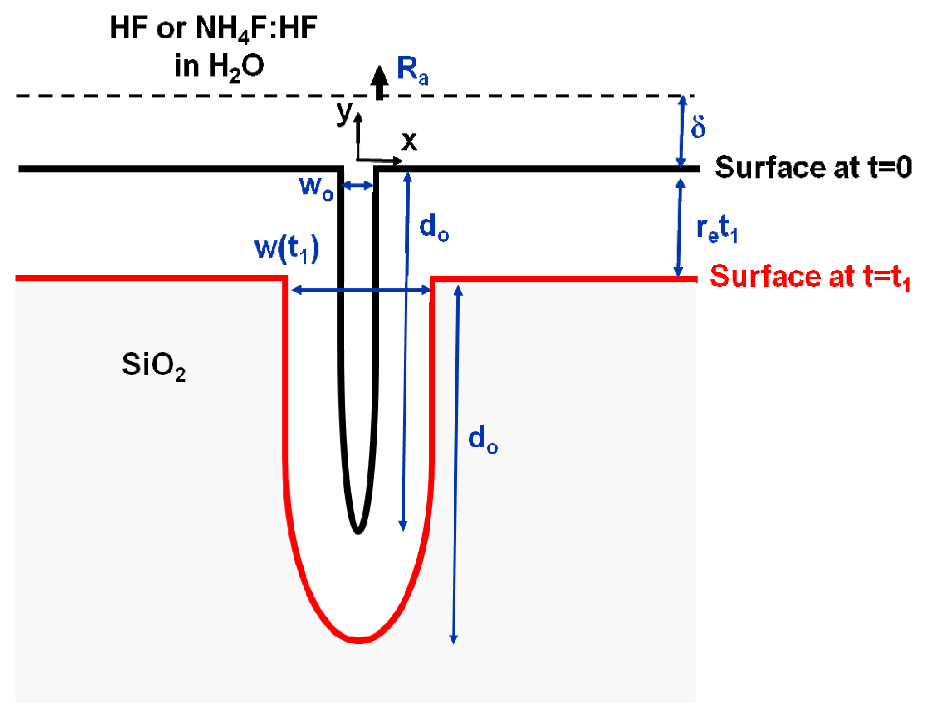

Governing Equations

$$\boxed{\frac{\partial C(x,y,t)}{\partial t} = D\,\nabla^2 C(x,y,t)}$$

$$\boxed{\frac{\partial C(x,\delta,t)}{\partial x} = \frac{k_c(t)\left(C(x,\delta,t) - C_{oo}\right)}{D}}$$

Convective mass transfer from top of crack (R_a)

$$\boxed{\begin{array}{ll} C(surface,t) = C_s & (etch) \\ \dfrac{dC(surface,t)}{dn} = 0 & (rinse) \end{array}}$$

Source from crack (R_b)

Power spectra from Monte Carlo polishing simulations show good agreement with power spectra of measured polished surfaces

11/23/12

Unstabilized Hastilite Polished Surface

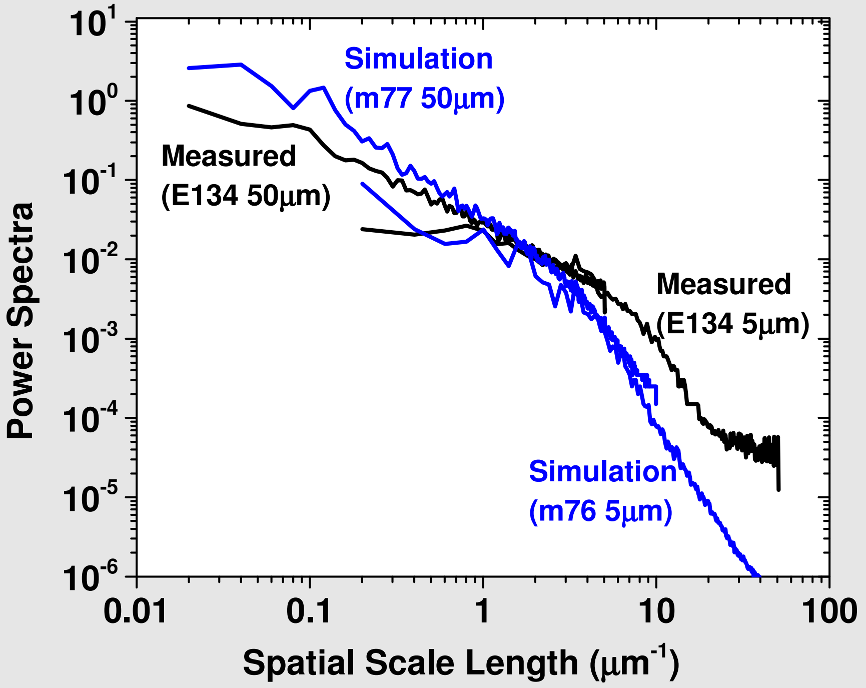

Stabilized Hastilite Polished Surface

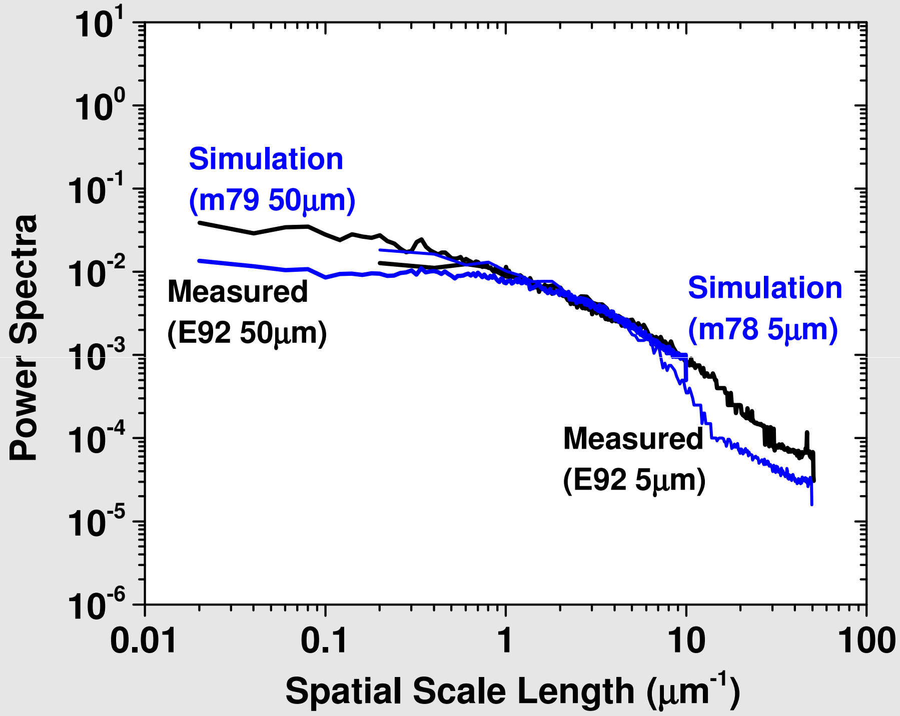

dr=1nm; mol removal=0.04 nm

Coupled thermo-mechanical finite element analysis was used to model laser heating of fused silica (T<2300K)

Thermal transport

$$\rho C_p \frac{\partial T}{\partial t} = \nabla \cdot \left(k \nabla T\right) + Q$$

$$Q = \frac{\alpha P}{\pi r_0^2} \exp\left(-\frac{2r^2}{r_0^2} - \alpha z\right)$$

Viscoelasticity

$$\nabla \cdot \sigma + b = \rho \frac{\partial^2 u}{\partial t^2}$$

$$\dot{\varepsilon}' = \frac{\sigma'}{\eta_o \cdot e^{\frac{\Delta H}{RT(t)}}} + \frac{\dot{\sigma}'}{2 \cdot G}$$

Volume relaxation

$$T_f = T - \int_0^t M(t) \frac{\partial T}{\partial t'} dt'$$

$$M(t) = e^{-(t/\tau_s)^{\beta}} = \sum_k e^{-(t/\tau_{sk})}$$

Marangoni effect

$$M_a' = \frac{\sigma_M}{\sigma_V} = \frac{d\gamma}{dT} \frac{\tau_{\exp} \Delta T}{\eta r_0}$$

$$\sigma_M = \frac{d\gamma}{dT} \frac{\partial T}{\partial r} \approx \frac{d\gamma}{dT} \frac{T - T_0}{r_0}$$

Temperature & Displacement

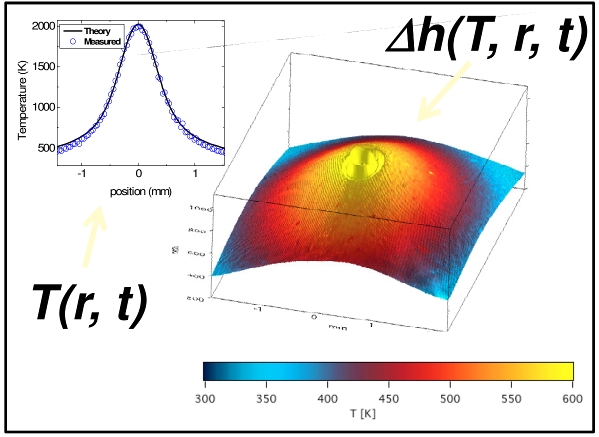

Stress & Densification

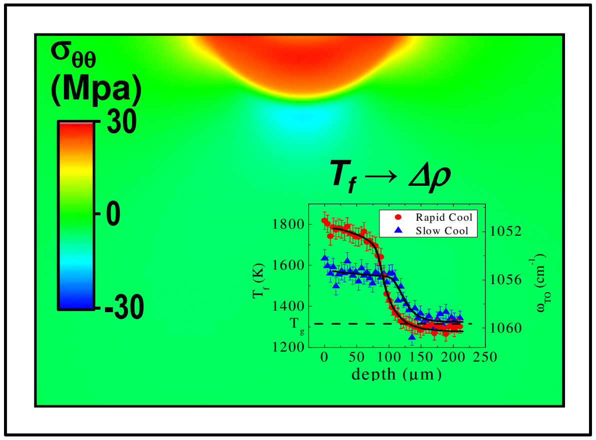

Surface Deformation & Flow

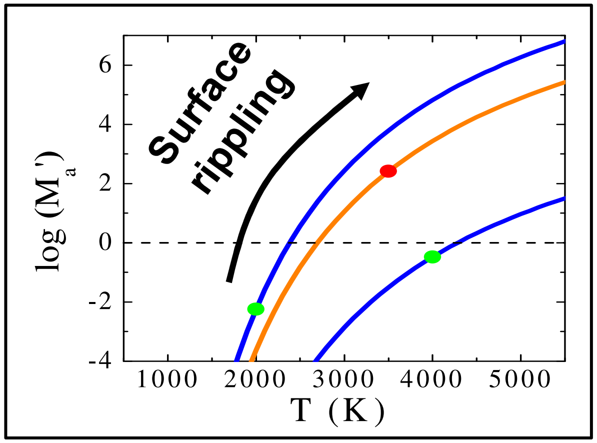

We have developed predictive physical models for laser-driven material response associated with damage mitigation

R. Vignes, JAC (in press) (2012); S. Yang, J. Appl. Phys. **106**, 1031061 (2009); N. Shen, Appl Surf Sci **256**, 4031(2010); M. Matthews, SPIE 7504 (2009); M. Matthews, Optics Letters **35**, 1-3 (2010)

Expressions for the crack depth and effective particle size distribution as function of the crack length distribution have been derived

Crack Depth Distribution

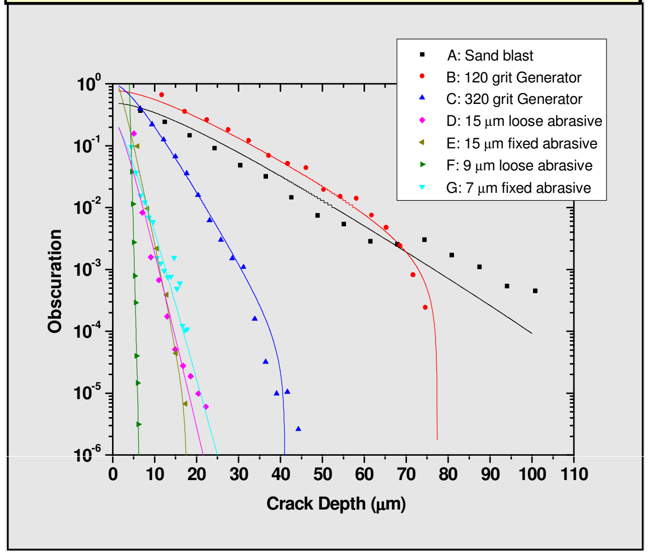

Calculated effective particle size distribution

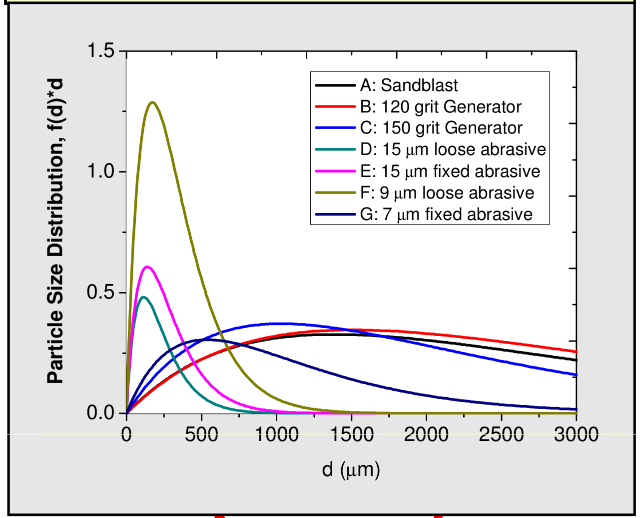

Crack Length Distribution

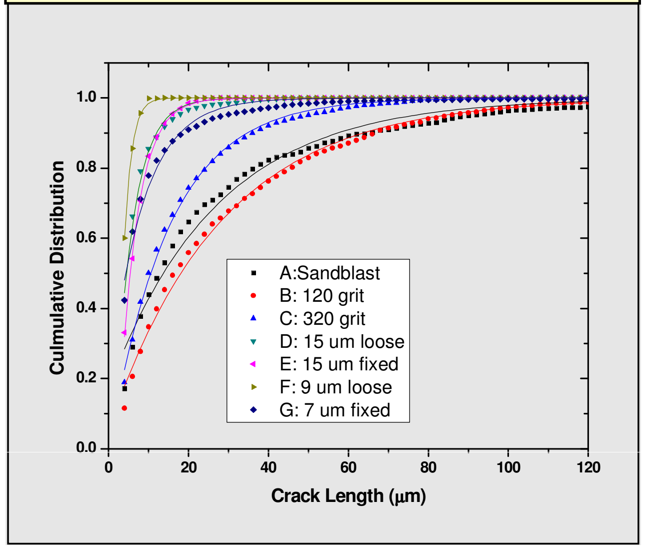

$$c = \left(\frac{x_h}{K_{Ic}} P \right)^{\frac{2}{3}}$$

↔

$$P(d) = \frac{P_T}{N_L} \left(\frac{d}{d_c} \right)$$

↔

$$L \cong \frac{\pi}{2} \left(\frac{2}{3} \frac{k}{E_s} P\, d \right)^{\frac{1}{3}}$$

$$d(L) = L^{3/2} \left(\frac{2}{\pi} \right)^{3/2} \left(\frac{3EN_L d_c}{2kP_T} \right)^{1/2}$$

Characteristic abrasive size (normalizing constant

$$c(L) = \frac{L}{\frac{\pi}{2} \left(\frac{K_{Ic}}{\chi_h} \right)^{2/3} \left(\frac{2k\, N_L d_c}{3E\, P_T} \right)^{1/3}} = \frac{L}{\Omega}$$

Note the crack depth and crack length are linearly related for a constant Ω

The effect of load on the fracture behavior of scratches has been measured

Schematic description of fractures associated with a scratch

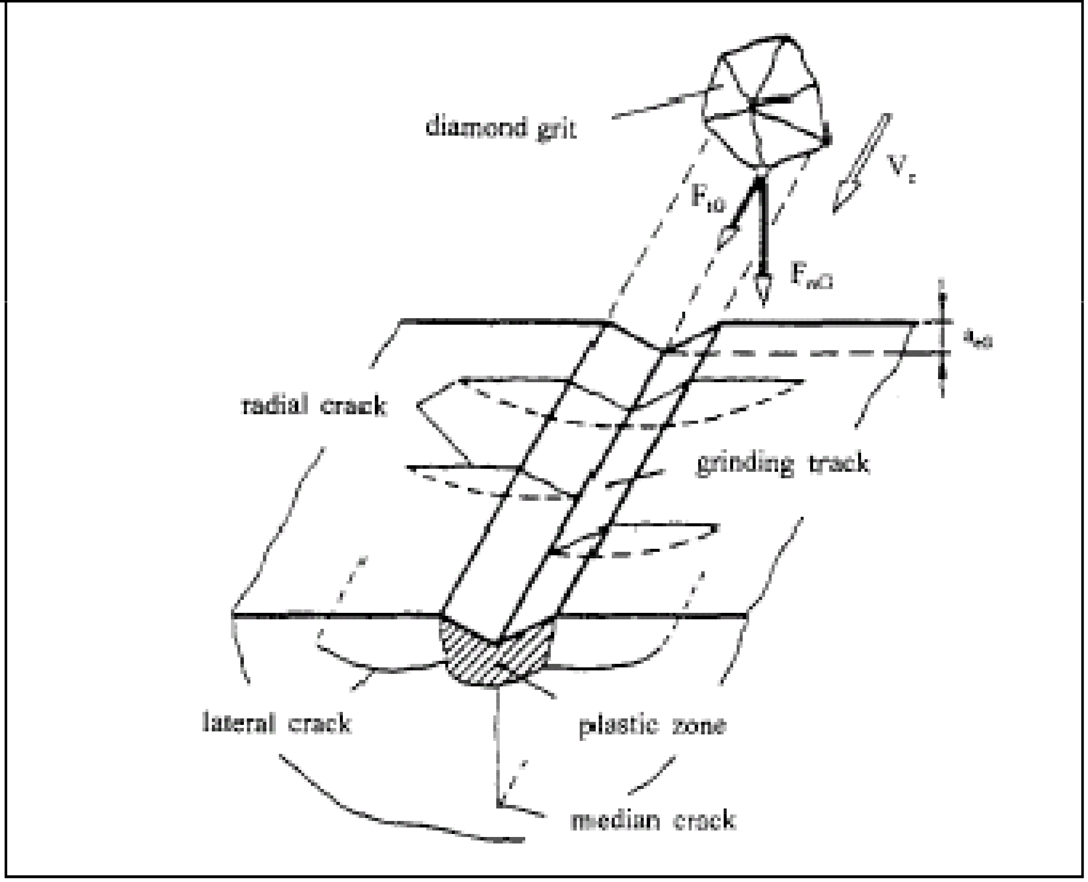

- **At low loads (P<0.1 N),** no cracking is observed just a ductile track
- **At intermediate loads (0.1 N< P < 5 N),** well defined median and lateral cracks form
- **At high loads (P> 5N),** the plastically observed track appears to shatter and the median and lateral crack are not as extending as in the higher end of the intermediate loads

K. Li, J. of Mat. Proc. Tech. 57 (1996); M. Swain, Proc. R. Soc. London A, 366 (1979) 575

SurF model predicts convergence and convergence rate without any fitting parameters